Article

Neuron

The Sorting Receptor SorCS1 Regulates Trafficking of Neurexin and AMPA Receptors

Highlights

- Proteomics identifies neurexins and AMPA receptors as key proteins sorted by SorCS1
- SorCS1 regulates surface levels of neurexin and AMPA receptors
- SorCS1 maintains synaptic abundance of adhesion proteins and AMPA receptors in vivo
- Impaired AMPA receptor trafficking in the absence of SorCS1 reduces synaptic transmission

Authors

Jeffrey N. Savas, Luís F. Ribeiro, Keimpe D. Wierda, ..., John R. Yates III, Anirvan Ghosh, Joris de Wit

Correspondence

jyates@scripps.edu (J.R.Y.), joris.dewit@cme.vib-kuleuven.be (J.d.W.)

In Brief

The formation, function, and plasticity of synapses require changes in receptor composition. Savas et al. identify the sorting receptor SorCS1 as a major regulator of receptor trafficking and show that SorCS1 maintains synaptic levels of key adhesion and neurotransmitter receptors.

Savas et al., 2015, Neuron *87*, 764–780
August 19, 2015
http://dx.doi.org/10.1016/j.neuron.2015.08.007

CellPress

CellPress

Neuron
Article

The Sorting Receptor SorCS1 Regulates Trafficking of Neurexin and AMPA Receptors

Jeffrey N. Savas,[1,5] Luís F. Ribeiro,[2] Keimpe D. Wierda,[2] Rebecca Wright,[3] Laura A. DeNardo-Wilke,[3] Heather C. Rice,[2] Ingrid Chamma,[4] Yi-Zhi Wang,[5] Roland Zemla,[6] Mathieu Lavallée-Adam,[1] Kristel M. Vennekens,[2] Matthew L. O'Sullivan,[3] Joseph K. Antonios,[3] Elizabeth A. Hall,[5] Olivier Thoumine,[4] Alan D. Attie,[7] John R. Yates III,[1,*] Anirvan Ghosh,[3,8] and Joris de Wit[2,*]

[1]Department of Chemical Physiology, The Scripps Research Institute, La Jolla, CA 92037, USA
[2]VIB Center for the Biology of Disease, 3000 Leuven, Belgium; Center for Human Genetics, KU Leuven, 3000 Leuven, Belgium
[3]Neurobiology Section, Division of Biology, University of California, San Diego, La Jolla, CA 92093, USA
[4]UMR 5297, Interdisciplinary Institute for Neuroscience, University of Bordeaux and Centre National de la Recherche Scientifique, 33000 Bordeaux, France
[5]Department of Neurology, Feinberg School of Medicine, Northwestern University, Chicago, IL 60611, USA
[6]School of Medicine, New York University, New York, New York 10016, USA
[7]Department of Biochemistry, University of Wisconsin-Madison, Madison, WI 53706, USA
[8]Neuroscience Discovery, F. Hoffman-La Roche, 4070 Basel, Switzerland
*Correspondence: jyates@scripps.edu (J.R.Y.), joris.dewit@cme.vib-kuleuven.be (J.d.W.)
http://dx.doi.org/10.1016/j.neuron.2015.08.007

SUMMARY

The formation, function, and plasticity of synapses require dynamic changes in synaptic receptor composition. Here, we identify the sorting receptor SorCS1 as a key regulator of synaptic receptor trafficking. Four independent proteomic analyses identify the synaptic adhesion molecule neurexin and the AMPA glutamate receptor (AMPAR) as major proteins sorted by SorCS1. SorCS1 localizes to early and recycling endosomes and regulates neurexin and AMPAR surface trafficking. Surface proteome analysis of *SorCS1*-deficient neurons shows decreased surface levels of these, and additional, receptors. Quantitative in vivo analysis of *SorCS1*-knockout synaptic proteomes identifies SorCS1 as a global trafficking regulator and reveals decreased levels of receptors regulating adhesion and neurotransmission, including neurexins and AMPARs. Consequently, glutamatergic transmission at *SorCS1*–deficient synapses is reduced due to impaired AMPAR surface expression. *SORCS1* mutations have been associated with autism and Alzheimer disease, suggesting that perturbed receptor trafficking contributes to synaptic-composition and -function defects underlying synaptopathies.

INTRODUCTION

Proper formation and function of synapses require the coordinated assembly of large and heterogeneous protein complexes on the pre- and postsynaptic side. The composition of the synaptic proteome varies with synaptic neurotransmitter type and developmental stage, changes upon activity-induced changes in synaptic strength, and is affected in synaptopathies (Cajigas et al., 2010; Grant, 2012).

Receptors are core components of the synaptic proteome. Their dynamic trafficking is a key feature underlying the function and plasticity of synapses (Choquet and Triller, 2013). The transport and synaptic insertion and removal of AMPA glutamate receptors (AMPARs), for example, are tightly regulated in order to control synaptic efficacy (Shepherd and Huganir, 2007). Adhesion molecules are another key class of synaptic receptors (Giagtzoglou et al., 2009). Neurexin (Nrxn) presynaptic adhesion molecules play a central role in the formation, maturation, and plasticity of synapses (Krueger et al., 2012). Nrxns interact with distinct postsynaptic adhesion molecules, including neuroligins (Nlgns) and LRRTMs (de Wit et al., 2009; Dean et al., 2003; Graf et al., 2004; Ichtchenko et al., 1995; Ko et al., 2009; Scheiffele et al., 2000; Siddiqui et al., 2010). Some adhesion molecules, such as the LRRTMs, also interact with AMPARs (de Wit et al., 2009; Schwenk et al., 2012). Furthermore, presynaptic Nrxn regulates postsynaptic AMPAR trafficking via a *trans*-synaptic interaction with Nlgns and LRRTMs (Aoto et al., 2013). Adhesion molecules and neurotransmitter receptors are thus closely linked and are key components of the synaptic machinery. However, in contrast to AMPARs, little is known about the mechanisms regulating adhesion molecule trafficking.

As core synaptic receptors, adhesion molecules and AMPARs might be co-regulated. To test this idea, we took Nrxn as a central synaptic component, screened for Nrxn-interacting proteins with a role in trafficking, and then determined whether that mechanism is shared more broadly among other synaptic receptors. We identified the VPS10P sorting receptor SorCS1 as a Nrxn-interacting protein. Vacuolar protein sorting 10 (VPS10P)-receptor-family proteins are important regulators of intracellular trafficking (Hermey, 2009; Willnow et al., 2008). The mammalian VPS10P receptors Sortilin and SorLA sort cargo proteins in Golgi-to-endosome trafficking pathways (Nielsen et al., 2007; Nielsen et al., 2001). Less is known about the sorting function and endogenous cargo of the three remaining mammalian

VPS10P receptors, SorCS1–SorCS3 (sortilin-related CNS expressed). *SorCS* genes are expressed in complementary patterns in the brain (Hermey et al., 2004; Oetjen et al., 2014) and have been associated with autism, schizophrenia, bipolar disorder, attention deficit hyperactivity disorder, and late-onset Alzheimer disease (Christoforou et al., 2011; Grupe et al., 2006; Lionel et al., 2011; Ollila et al., 2009; Reitz et al., 2011; Sanders et al., 2012). The prominent association of *SORCS* genes with synaptopathies and the discovery of SorCS receptors in a Nrxn-interactor screen suggest that SorCS proteins might play a role in the trafficking of synaptic components.

Here, we identify Nrxn and AMPARs as key synaptic proteins sorted by SorCS1. SorCS1 localizes to early and recycling endosomal compartments and regulates surface trafficking of Nrxn and AMPARs. SorCS1 interactome analysis reveals close association with several synaptic proteins, including Nrxn, Nlgn, and AMPARs. Quantitative surface proteome analysis reveals reduced surface expression of these proteins in *SorCS1*-deficient neurons. In vivo quantitative analysis of *SorCS1*-knockout synaptic proteomes shows decreased abundance of receptors, including Nrxns and AMPARs, regulating adhesion and synaptic transmission. Loss of *SorCS1* reduces glutamatergic synaptic transmission as a result of impaired surface expression of AMPARs at excitatory synapses. Together, our results identify SorCS1 as a major trafficking regulator of receptors that are essential for synaptic function.

RESULTS

Identification of SorCS1 as a Nrxn-Binding Protein

To discover Nrxn-interacting proteins, we used a combination of affinity chromatography with Nrxn ectodomains and mass spectrometric (MS) analysis (Savas et al., 2014) (Figure 1A). We purified recombinant Nrxn1β-Fc proteins lacking or containing splice site 4 (Nrxn1β[− or +SS4]-Fc) (Figure S1A), the best-characterized Nrxn splice site in terms of protein interactions (Krueger et al., 2012), and used these to identify interacting proteins in detergent-solubilized rat-brain homogenate. We identified Nlgn1–Nlgn3 as Nrxn-binding proteins with a preference for Nrxn1β(−SS4)-Fc (Figure 1B) (Boucard et al., 2005) and identified LRRTM1 as a Nrxn1β(−SS4)-Fc-specific interactor (Ko et al., 2009; Siddiqui et al., 2010) (Table S1), validating our approach.

Strikingly, the two most abundant Nrxn1β-interacting proteins identified in this experiment were the VPS10P sorting receptor proteins SorCS1 and SorCS2 (Figure 1B). The identification of SorCS proteins as candidate Nrxn interactors was particularly interesting, given that these have not previously been identified as Nrxn-binding proteins and might be involved in regulating Nrxn trafficking. SorCS1 and SorCS2 are members of the VPS10P family, which regulates intracellular trafficking and neuronal function (Hermey, 2009; Willnow et al., 2008), but the endogenous cargo and trafficking functions of SorCS proteins are not well understood. To determine whether Nrxn also interacts with SorCS at synapses, we repeated our affinity chromatography experiment by using synaptosome extracts and again identified Nlgn1–Nlgn3 and SorCS1 and SorCS2 as the most abundant Nrxn1β-interacting proteins (Figures 1C and 1D; Table S1). The other mammalian VPS10P receptors Sortilin and SorLA were not identified in these experiments (Table S1). The interaction of Nrxn1β with SorCS was lost at high detergent concentrations, whereas the interaction with Nlgns was not (Figure S1B), suggesting that the Nrxn1β-SorCS complex is less stable than Nrxn1β-Nlgn. Finally, affinity purifications with an antibody against the common Nrxn cytoplasmic domain independently identified SorCS1 (Figure S1C). These experiments suggest that SorCS1 is a novel endogenous Nrxn-binding partner.

To verify the MS results, we carried out a series of binding assays. We expressed SorCS1cβ-myc in HEK293T cells and applied Nrxn1β(− or +SS4)-Fc to assess surface binding. Both Nrxn1β-Fc proteins bound to SorCS1 and the positive control Nlgn1, whereas Fc alone showed no detectable binding (Figure 1E). Rather than labeling the cell surface, Nrxn1β-Fc clustered in large intracellular puncta (Figure 1E), suggesting internalization of Nrxn1β by SorCS1. In reciprocal experiments, SorCS1-ecto-His strongly bound to cells expressing Nrxn1β-CFP but not to cells expressing GFP (Figure S1D). Complementary pulldown assays with transfected HEK cell lysates confirmed the SorCS1-Nrxn1β interaction (Figures S1E and S1F). Direct binding assays demonstrated that SorCS1-ecto-His coprecipitated with Nrxn1β-Fc but not with the control proteins LPHN3-Fc (O'Sullivan et al., 2012) or Fc alone (Figure 1F), showing a direct interaction between the SorCS1 and Nrxn1β ectodomains.

To estimate the affinity of the interaction, we measured SorCS1-Nrxn1β cell surface binding. Scatchard analysis indicated a Kd = 2.22 ± 0.87 nM after subtracting non-specific binding to control cells (Figure 1G), demonstrating an apparent high-affinity binding of SorCS1 to cell surface Nrxn1β. To identify the domain in SorCS1 required for Nrxn1β binding, we analyzed Nrxn1β-Fc binding to full-length (FL) SorCS1cβ and to SorCS1 mutants lacking the pro-peptide domain (ΔPRO), the ligand-binding VPS10P domain (ΔVPS), the polycystic kidney disease domain (ΔPKD), or the leucine-rich domain (ΔLRD) (Figure 1H). Surface expression was confirmed for all SorCS1 mutants (Figure S1G). Deletion of the VPS10P domain abolished SorCS1 binding to Nrxn1β in both pulldown (Figure 1I) and surface-binding assays (Figure 1J). Together, these results show that the SorCS1-Nrxn1β interaction is direct, has high affinity, and requires the VPS10P domain.

SorCS1 Localizes to Endosomal Compartments and Excitatory Synapses

The identification of SorCS1 as a Nrxn interactor suggests that SorCS1 may localize to synapses. Punctate SorCS1 immunoreactivity has been observed in neuronal cell bodies and dendrites (Hermey et al., 2001), but the nature of these SorCS1-positive compartments is unclear. To gain insight into the subcellular localization of SorCS1, we first labeled HeLa cells expressing HA-SorCS1cβ with a panel of antibodies for intracellular compartments. SorCS1 displayed a punctate distribution throughout the cytoplasm, where it partially colocalized with the early endosome marker EEA1 (Figure 2A). Robust colocalization was observed with Alexa 568-transferrin (Tf; 30 min uptake) (Figure 2B) and with the transferrin receptor (TfR; Figure S2A). SorCS1 also colocalized with the recycling endosome marker

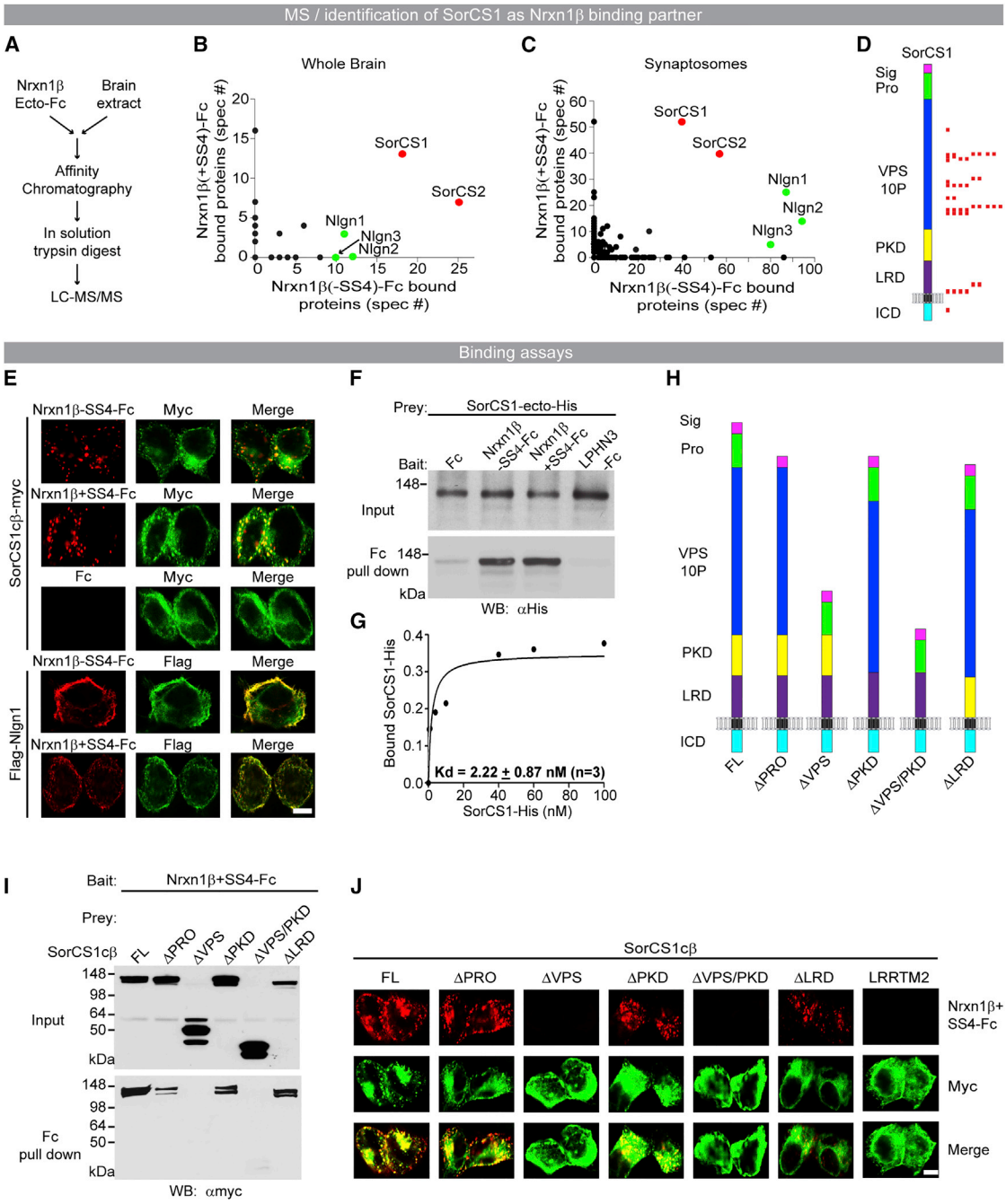

Figure 1. Identification of SorCS1 as a Nrxn-Binding Protein

(A) Proteomic workflow for the identification of Nrxn1β-interacting proteins

(B) Frequency of detection of all peptides (total spectra count) for proteins identified in both Nrxn1β(+SS4)-Fc and Nrxn1β(−SS4)-Fc affinity purifications after background (Fc alone) subtraction with whole-brain prey extracts.

(C) Nrxn1β-Fc affinity purification as in (B) with synaptosome prey extracts.

(D) SorCS1 protein domain organization with mapped peptide MS identifications (red) from synaptosome prey experiment with Nrxn1β(+SS4) bait. Sig, signal peptide; Pro, pro-peptide; VPS10P, vacuolar protein sorting 10 protein; PKD, polycystic kidney disease domain; LRD, leucine-rich domain; ICD, intracellular domain.

(E) Surface-binding experiments with Nrxn1β-Fc or control Fc on HEK293T cells expressing SorCS1cβ-myc or FLAG-Nlgn1.

(F) Direct binding assay with Fc proteins and SorCS1-ecto-His.

(G) Estimation of SorCS1/Nrxn1β binding affinity. Representative experiment demonstrating concentration-dependent SorCS1-ecto-His binding to FLAG-Nrxn1β(−SS4)-expressing HEK cells (n = 3 independent experiments).

(legend continued on next page)

Rab11 and the *trans* Golgi network marker TGN-46, but displayed little overlap with the late endosomal marker CD63 or the lysosomal marker LAMP1 (Figures 2C and S2B–D). These observations suggest that SorCS1 localizes to endosomal recycling compartments in HeLa cells.

To determine the subcellular localization of SorCS1 in neurons, we tested a wide panel of commercially available and custom-made SorCS1 antibodies but found that none were suitable for the immunocytochemical detection of SorCS1 (data not shown). We therefore expressed epitope-tagged SorCS1cβ in cultured neurons. SorCS1 displayed a punctate distribution in cell body and dendrites. Quantification of the intensity of SorCS1 fluorescence in axons and dendrites showed a distribution comparable to that of the somatodendritic marker TfR-GFP (Farías et al., 2012), indicating that SorCS1 predominantly localizes to the somatodendritic compartment (Figures 2D–2G). In dendrites, SorCS1 puncta colocalized with EEA1, Alexa 568-Tf (60 min uptake) (Figures 2H, 2I, and 2K), and TfR (Figures 2K and S2E), but showed less overlap with TGN-46, CD-63, or LAMP1 (Figures 2K and S2F–S2H). Co-expression of SorCS1 and Rab-GFP constructs for labeling different endosomal compartments revealed the highest overlap of SorCS1 with the early and recycling endosome markers Rab4, Rab5, and Rab11, but not with the late endosome marker Rab7 (Figurse 2L and S2JN–S2M). These results indicate that SorCS1 localizes to endosomal compartments in dendrites and spines.

We next compared the localization of SorCS1 to synaptic markers. SorCS2 and SorCS3 are postsynaptic density proteins (Bayés et al., 2012; Breiderhoff et al., 2013), suggesting that SorCS1 might also be synaptic. SorCS1 colocalized with the excitatory postsynaptic marker PSD95 in dendritic spines (Figures 2J and 2K) and was juxtaposed to the presynaptic marker VGluT1 (Figures 2K and S2I). Subcellular fractionation (Figure S2N) with a verified SorCS1 antibody (Figures S2O–S2Q) showed SorCS1 immunoreactivity in purified postsynaptic density fractions, which contained PSD95. Little SorCS1 was detected in the presynaptic fraction containing synaptophysin. Thus, SorCS1 predominantly localizes to early and recycling endosomes, consistent with a role in sorting cargo proteins. In addition, SorCS1 can be detected at the postsynaptic density of glutamatergic synapses.

SorCS1 Regulates the Cell Surface Distribution of Nrxn

The endosomal localization of SorCS1 is consistent with a role in the intracellular sorting of cargo proteins and the regulation of receptor surface distribution. If SorCS1 regulates the cell surface distribution of Nrxn, SorCS1 and Nrxn would be expected to colocalize. SorCS1 localizes to the somatodendritic compartment (Figure 2D-G), whereas Nrxn predominantly functions presynaptically. However, several studies have reported additional dendritic localization of Nrxn (Berninghausen et al., 2007; Fairless et al., 2008; Taniguchi et al., 2007). We first assessed SorCS1 and Nrxn localization and found that both proteins colocalized in endosomes in HeLa cells and in dendrites (Figures S3A–S3C), corroborating previous results demonstrating localization of Nrxn1β in dendritic endosomes (Taniguchi et al., 2007). Subcellular fractionation further indicated a pool of endogenous Nrxn in the postsynaptic fraction (Figure S2N), confirming previous observations (Berninghausen et al., 2007). Their endosomal colocalization suggests that SorCS1 and Nrxn might preferentially interact in *cis*. To test whether SorCS1 and Nrxn interact in *cis* or in *trans*, we performed antibody-mediated aggregation experiments and found that clustering of SorCS1 resulted in VPS10P domain-dependent coaggregation of Nrxn1β or vice versa (Figure S3D). Coculture assays for testing whether SorCS1 might also interact with Nrxn in *trans* did not support a *trans* interaction (Figures S3E–S3G), indicating a preferential *cis* interaction of SorCS1 and Nrxn.

To determine whether SorCS1 regulates Nrxn surface levels, we first overexpressed SorCS1cβ-myc (FL or ΔVPS) in hippocampal neurons. These neurons express *SorCS2* and *SorCS3* but express *SorCS1* at very low levels or not at all (Hermey et al., 2004; Oetjen et al., 2014). We tested multiple Nrxn antibodies but none of these proved suitable for the detection of endogenous cell surface Nrxn (data not shown). We therefore expressed Nrxn1β(−SS4) tagged with an extracellular epitope (SEP-Nrxn1β) to analyze Nrxn surface levels. Overexpression of SorCS1 FL, but not of SorCS1 ΔVPS, significantly decreased the ratio of surface/total SEP-Nrxn1β in dendrites in comparison to that in control cells (Figures 3A and 3B). We next tested the effect of loss of *SorCS1* on dendritic Nrxn surface levels. We cultured cortical neurons, which strongly express *SorCS1* (Hermey et al., 2004; Oetjen et al., 2014), from *SorCS1*$^{flox/flox}$ mice (Lane et al., 2010) and expressed Cre recombinase in these cells to reduce *SorCS1* levels. Compared to that in control cells, the surface/total SEP-Nrxn1β ratio was significantly increased in *SorCS1* KO dendrites (Figures 3C and 3D). This increase in surface/total SEP-Nrxn1β ratio was due to both an increase in SEP-Nrxn1β dendritic surface intensity (Figure 3E) and a small decrease in SEP-Nrxn1β total intensity in *SorCS1* KO dendrites (Figure 3F). These results indicate that overexpression of SorCS1 decreases, whereas loss of *SorCS1* increases, dendritic Nrxn surface levels.

Although Nrxn is present on the dendritic surface, the majority of Nrxn is expressed on the axonal surface (Fairless et al., 2008), which is functionally the most important site for Nrxns. To determine whether loss of *SorCS1* might also affect axonal Nrxn surface levels, we analyzed the SEP-Nrxn1β surface/total ratio in *SorCS1*-deficient axons. We observed strong SEP-Nrxn1β surface expression in control axons (Figure 3G) and found that the surface/total SEP-Nrxn1β ratio was significantly decreased in *SorCS1* KO axons (Figures 3G and 3H). This decrease underestimates the extent of downregulation of axonal Nrxn surface expression in *SorCS1* KO neurons because we observed both a robust decrease in axonal SEP-Nrxn1β surface intensity (Figure 3I) and a decrease in total SEP-Nrxn1β

(H) SorCS1 deletion mutants.

(I) Pulldown experiment with Nrxn1β(+SS4)-Fc on HEK cell lysates transfected with SorCS1 deletion constructs.

(J) Binding of Nrxn1β(+SS4)-Fc to HEK cells expressing SorCS1 deletion constructs or myc-LRRTM2 as a control. Scale bars in (E) and (J), 10 μm. See also Figure S1.

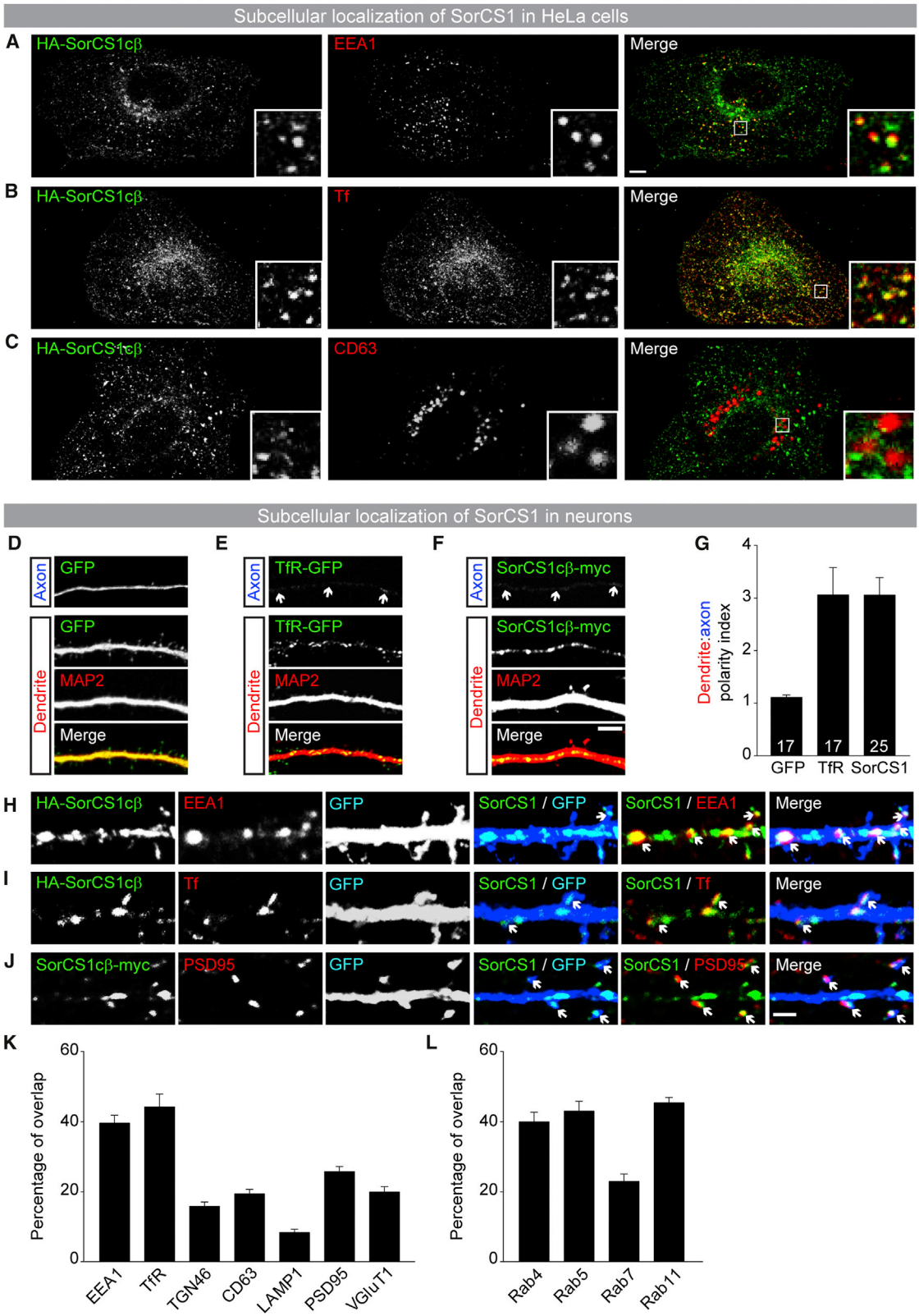

Figure 2. SorCS1 localizes to endosomal compartments and excitatory synapses.
(A–C) SorCS1 localization in HeLa cells.

(legend continued on next page)

intensity (Figure 3J). Together, these results show that SorCS1 controls Nrxn surface distribution in neurons in a compartment-specific manner: SorCS1 overexpression removes Nrxn from the dendritic surface, whereas *SorCS1* KO results in Nrxn accumulation on the dendritic surface and a loss of Nrxn from the axonal surface.

Because the total Nrxn intensity is decreased in *SorCS1* KO neurons (Figures 3F and 3J), we asked whether loss of *SorCS1* affects total Nrxn levels. We analyzed whole cell lysates of DIV14 (days in vitro) *SorCS1*$^{flox/flox}$ cortical neurons infected with a lentiviral vector encoding Cre recombinase (LV-Cre) by western blot and found a significant decrease in total Nrxn1β levels compared to those in control neurons (Figures 3K and 3L). To test whether Nrxn is degraded in *SorCS1* KO neurons, we quantified the overlap of SEP-Nrxn1β with the lysosomal marker LAMP1 and found a significantly increased overlap compared to that in control cells (Figures S3H and S3I), suggesting that Nrxn undergoes lysosomal degradation in the absence of SorCS1. Taken together, these results demonstrate that in the absence of SorCS1-mediated sorting, Nrxn is mis-sorted to the dendritic surface, lost from the axonal surface, and ultimately degraded.

SorCS1 Interactome Analysis Identifies Nrxns and Other Synaptic Receptors

As a sorting receptor, SorCS1 might regulate the surface trafficking of additional receptors besides Nrxn. To determine whether SorCS1 interacts with additional receptors, we characterized the molecular composition of the SorCS1 complex in the brain. We first performed affinity chromatography by using recombinant SorCS1-ecto-His as bait and detergent-solubilized synaptosome extract as prey, followed by MS analysis ("SorCS1-ecto MS"; Figure 4A). Coomassie staining showed an enrichment of proteins, which was absent when the SorCS1-ecto-His bait or the anti-His antibody were omitted, in the SorCS1-ecto-His pulldown lanes (Figure 4A). As expected, SorCS1-ecto MS detected Nrxn1 and Nrxn2 (Figures 4C and S4A; Table S2).

We identified multiple receptors, in addition to Nrxns, in the SorCS1 ectodomain interactome, several of which were synaptic. These included the synaptic adhesion molecules Nlgn1 and Nlgn3 (Figure 4C, 4D, and S4A; Table S2), and the AMPAR subunit Gria2 (GluA2) (Figure 4C and S4A; Table S2). Various other receptors were also present, including members of the Plexin semaphorin receptor family, the previously identified SorCS1 interactor amyloid precursor protein (APP) (Lane et al., 2010), and Ntrk2 (TrkB), the receptor for the neurotrophin BDNF (Table S2). The results from the SorCS1 ectodomain interactome analysis suggest that SorCS1 interacts with multiple receptors and may regulate key synaptic functions.

In a complementary approach, to also identify proteins interacting with the SorCS1 cytoplasmic tail, we affinity purified SorCS1 complexes from rat-brain extract by using two independent antibodies against SorCS1 (Figures S2O–S2Q) and a rabbit IgG control antibody, followed by LC-MS/MS analysis ("SorCS1 AP-MS"; Figure 4B). SorCS2 and SorCS3 were not detected in these samples (Table S3), supporting specificity of the antibodies used. Proteomic analysis of affinity-purified SorCS1 complexes revealed a prominent presence of adaptor protein (AP)-2-complex subunits (Figure S4B; Table S3), confirming previous findings (Nielsen et al., 2008). In addition to AP-2, which is important for clathrin-mediated endocytosis, the plasma-membrane clathrin-coat components Eps15 and epsins were also present in the SorCS1 complex (Figure S4B; Table S3), indicating that the SorCS1 cytoplasmic domain couples to the endocytic machinery. Confirming the SorCS1-ecto MS results, we again identified peptides for the synaptic adhesion molecules Nrxn2 and Nlgn3 and the AMPAR subunits Gria2 (GluA2) and Gria3 (GluA3) in the affinity-purified SorCS1 complex (Figures 4C, 4E, and S4B; Table S3). Together, these results show that SorCS1 complexes captured from brain-membrane extracts contain synaptic adhesion molecules and AMPA glutamate receptors.

Multiple Neuronal Receptors Depend on SorCS1 for Surface Trafficking

The presence of additional receptors besides Nrxn in the SorCS1 interactome suggests that SorCS1 may more broadly regulate receptor surface trafficking. To determine whether multiple receptors depend on SorCS1 for their surface trafficking, we performed a global, quantitative analysis of the surface proteome in control and *SorCS1*-deficient neurons by using stable isotope

(A) HA-SorCS1cβ (green) colocalizes with early endosome marker EEA1 (red).
(B) HA-SorCS1cβ colocalizes with internalized Alexa 568-transferrin (Tf) (red).
(C) HA-SorCS1cβ does not colocalize with late endosome marker CD63 (red).
(D–L) SorCS1 localization in neurons.
(D–G) DIV14 hippocampal neurons expressing GFP, TfR-GFP, or SorCS1cβ-myc were immunostained for MAP2 (dendritic marker; in red) and ankyrin G (axon initial segment marker; in blue, not shown) to determine SorCS1 somatodendritic versus axonal distribution. Shown are representative images with axonal and dendritic distribution of GFP (D), TfR-GFP (E), and SorCS1cβ-myc (F).
(G) Quantification of dendritic versus axonal distribution (D:A – polarity index) of GFP, TfR-GFP and SorCS1cβ. D:A = 1, uniform distribution in axons and dendrites; D:A < 1, preferential axonal distribution; and D:A > 1, preferential dendritic distribution. Number in bars indicates *n* for each condition in 3 independent experiments.
(H) HA-SorCS1cβ (green) coexpressed with GFP (blue) colocalizes with EEA1 (red) in dendrites and spines of hippocampal neurons (arrows).
(I) HA-SorCS1cβ colocalizes with Alexa 568-Tf (red) in dendrites and spines (arrows).
(J) SorCS1cβ-myc shows a partial overlap with postsynaptic excitatory marker PSD95 (red) in dendritic spines (arrows).
(K and L) Quantification of the colocalization of HA-SorCS1cβ with different markers in neurons in 3 independent experiments (n = 15 cells). Bar graphs show mean ± SEM. Scale bars in (A–C), 1 μm; scale bars in (D–F), 10 μm; scale bars in (H–J), 2 μm. See also Figure S2.

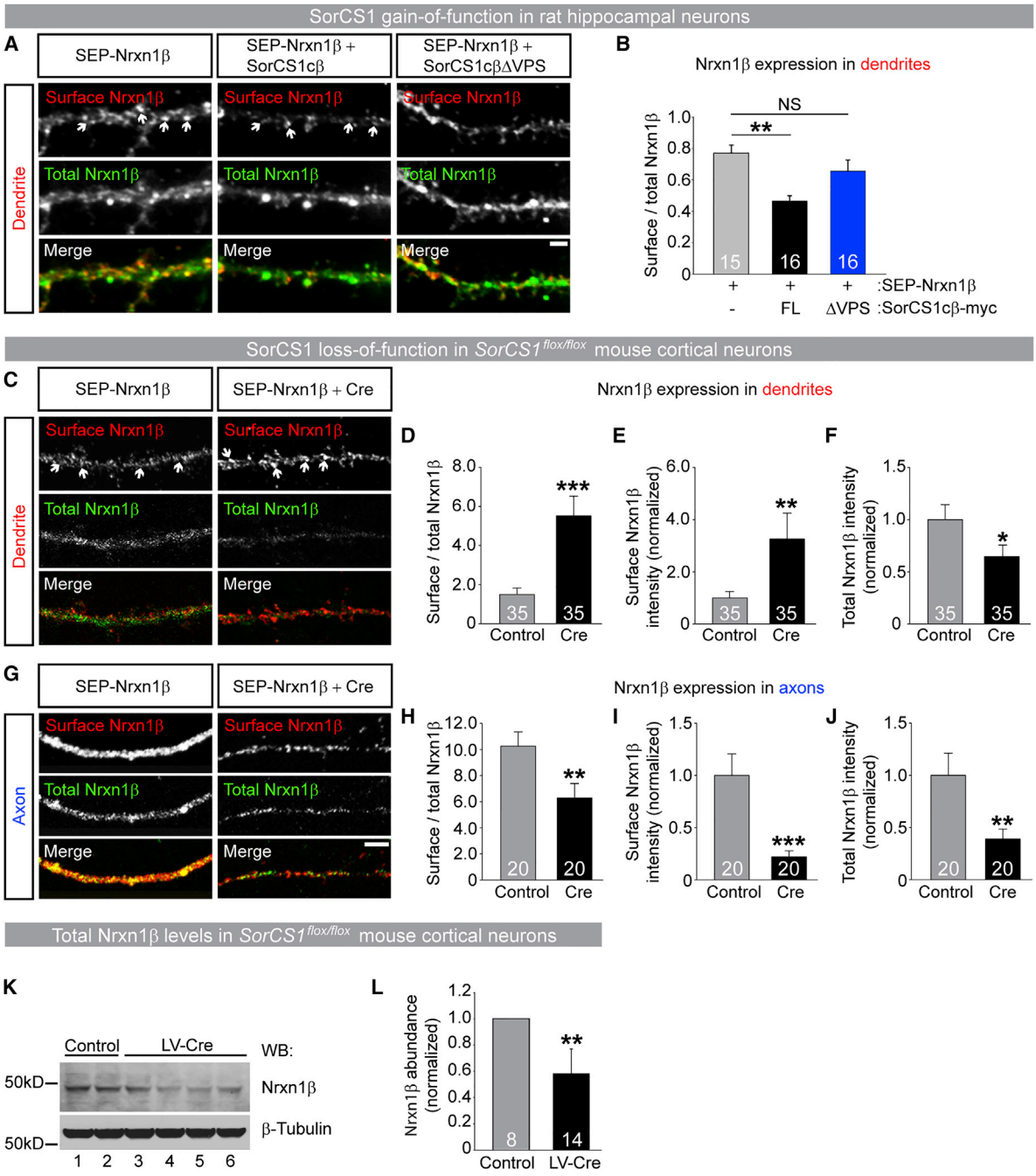

Figure 3. SorCS1 Regulates Nrxn Surface Distribution in Neurons

(A and B) SorCS1 gain-of-function experiments.

(A) Rat hippocampal neurons were co-transfected with SEP-Nrxn1β(−SS4) and an empty vector or SorCS1cβ-myc constructs and immunostained for GFP under non-permeabilizing conditions to label surface SEP-Nrxn1β. Overexpression of SorCS1cβ-myc full-length (FL), but not SorCS1β-myc ΔVPS, decreases dendritic Nrxn1β surface levels.

(B) Quantification of the dendritic Nrxn1β surface/total intensity ratio. **$p < 0.01$ by t test with non-parametric Mann-Whitney rank-sum test.

(C–L) *SorCS1* loss-of-function experiments.

(C) *SorCS1*$^{flox/flox}$ cortical neurons were co-electroporated with SEP-Nrxn1β(−SS4) and an empty vector (control) or Cre-myc (Cre). Loss of *SorCS1* increases dendritic Nrxn1β surface levels.

(D) Quantification of dendritic Nrxn1β surface/total intensity ratio.

(E) Loss of *SorCS1* increases dendritic Nrxn1β surface intensity.

(F) Dendritic Nrxn1β total intensity is reduced in *SorCS1* KO neurons.

(legend continued on next page)

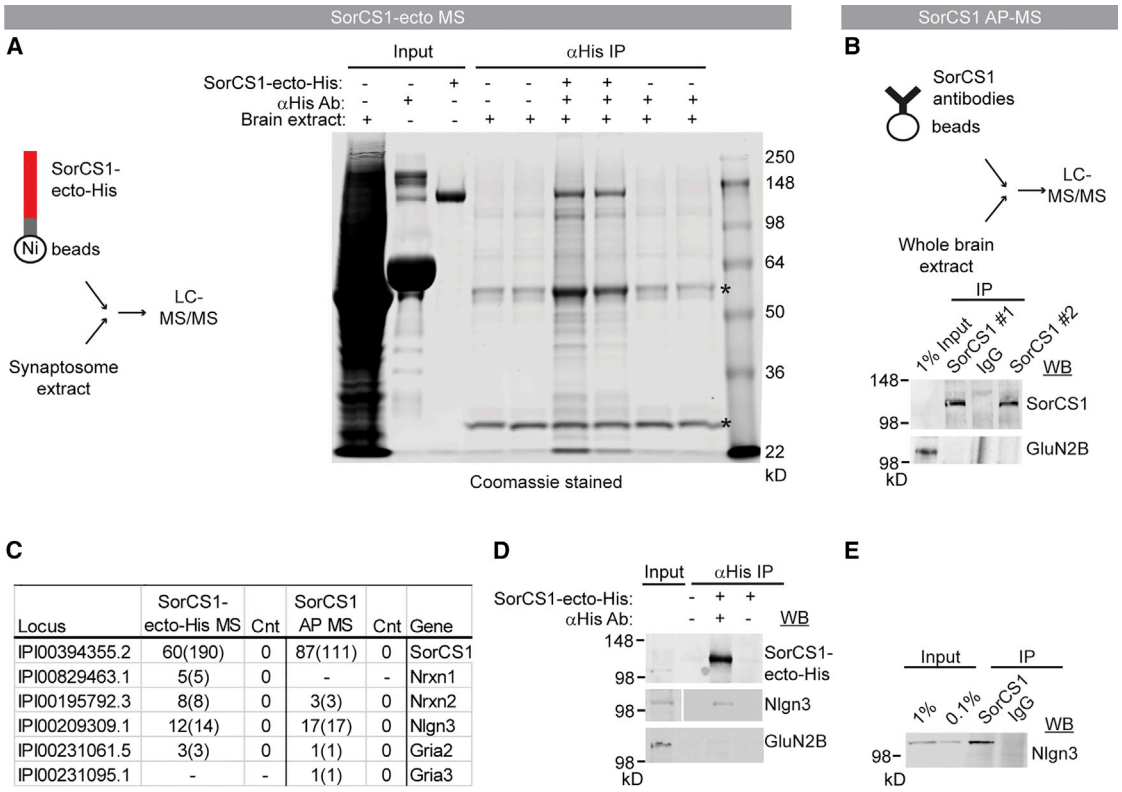

Locus	SorCS1-ecto-His MS	Cnt	SorCS1 AP MS	Cnt	Gene
IPI00394355.2	60(190)	0	87(111)	0	SorCS1
IPI00829463.1	5(5)	0	-	-	Nrxn1
IPI00195792.3	8(8)	0	3(3)	0	Nrxn2
IPI00209309.1	12(14)	0	17(17)	0	Nlgn3
IPI00231061.5	3(3)	0	1(1)	0	Gria2
IPI00231095.1	-	-	1(1)	0	Gria3

Figure 4. SorCS1 Interactome Analysis Identifies Synaptic Adhesion Molecules and AMPA Glutamate Receptors

(A) Schematic representation recombinant His-tagged SorCS1-ectodomain (SorCS1-ecto-His) interaction screen. Representative Coomassie-stained gel of proteins bound to bead-coupled SorCS1-ecto-His incubated with synaptosome extracts, with indicated negative control purifications. Asterisks indicate non-specific background bands.

(B) SorCS1 complex affinity-purification scheme. SorCS1 complexes were immunoprecipitated from whole postnatal rat-brain extracts with two independent SorCS1 antibodies and rabbit IgG controls. Western blot analysis of immunoprecipitated SorCS1 complexes with SorCS1 and GluN2B antibodies shows specific SorCS1 enrichment.

(C) MS summary table for SorCS1-ecto-His and SorCS1 affinity purifications (SorCS1-ecto-His MS and SorCS1 AP-MS, respectively). Indicated is the number of peptides and spectral counts (in parentheses) for each protein in both purification schemes with negative controls (see Tables S2 and S3 and Supplemental Experimental Procedures).

(D) Western blot validation for the recovery of the bait SorCS1-ecto-His and prey Nlgn3 proteins but not GluN2B.

(E) Western blot validation for the recovery of Nlgn3 in immunoprecipitated SorCS1 complexes. See also Figure S4.

labeling by amino acids in culture (SILAC). Cortical and hippocampal neurons were cultured from *SorCS1*$^{flox/flox}$ mice and divided into two sets. One set of control neurons was cultured in media containing stable heavy arginine and lysine isotopes and was mock infected ("heavy"); the other set of neurons was cultured in normal media and infected with LV-Cre ("light") to reduce SorCS1 levels (*SorCS1* cKO). The two sets of neurons were then surface biotinylated, lysed, mixed 1:1, and precipitated with neutravidin beads, followed by MS analysis ("*SorCS1* cKO surface SILAC analysis"; Figures 5A and S5A). We performed two independent experiments and quantified between 1,999 and 2,151 proteins from 7,869 and 10,146 peptides, respectively (Figures 5B and S5B–S5D). The corrected ratios (light/heavy) of the quantified peptides show a normal distribution with a tail representing peptides with a reduced ratio in *SorCS1* cKO cultures (Figure 5B), indicating a specific downregulation of surface proteins in *SorCS1* KO cultures.

Manual inspection of the raw MS1 mass-to-charge ratio (m/z) spectra indicated reduced surface levels of Nrxn1 and Nlgn3, whereas the surface abundance of the cell adhesion molecule Ncam1 was not affected (Figure 5C). We then graphed the light/heavy (*SorCS1* cKO/control) ratios for each experiment on

(G) Loss of *SorCS1* decreases axonal Nrxn1β surface levels.

(H) Quantification of axonal Nrxn1β surface/total intensity ratio.

(I) Loss of *SorCS1* reduces axonal Nrxn1β surface intensity.

(J) Axonal Nrxn1β total intensity is reduced in *SorCS1* KO neurons. *$p < 0.05$, **$p < 0.01$, and ***$p < 0.001$ by Mann-Whitney test. Bar graphs in (B), (D–F), and (H–J) show mean ± SEM; number in bars indicates *n* for each condition. Scale bars in (A), (C,) and (G), 5 μm.

(K) Extracts from DIV14 *SorCS1*$^{flox/flox}$ cortical neurons infected with LV-Cre at DIV2 show reduced Nrxn1β levels in comparison to those in control cells.

(L) Quantification of (K). **$p < 0.01$ by Student's t test. Bar graph shows mean ± STD; number in bars indicates *n* for each condition. See also Figure S3.

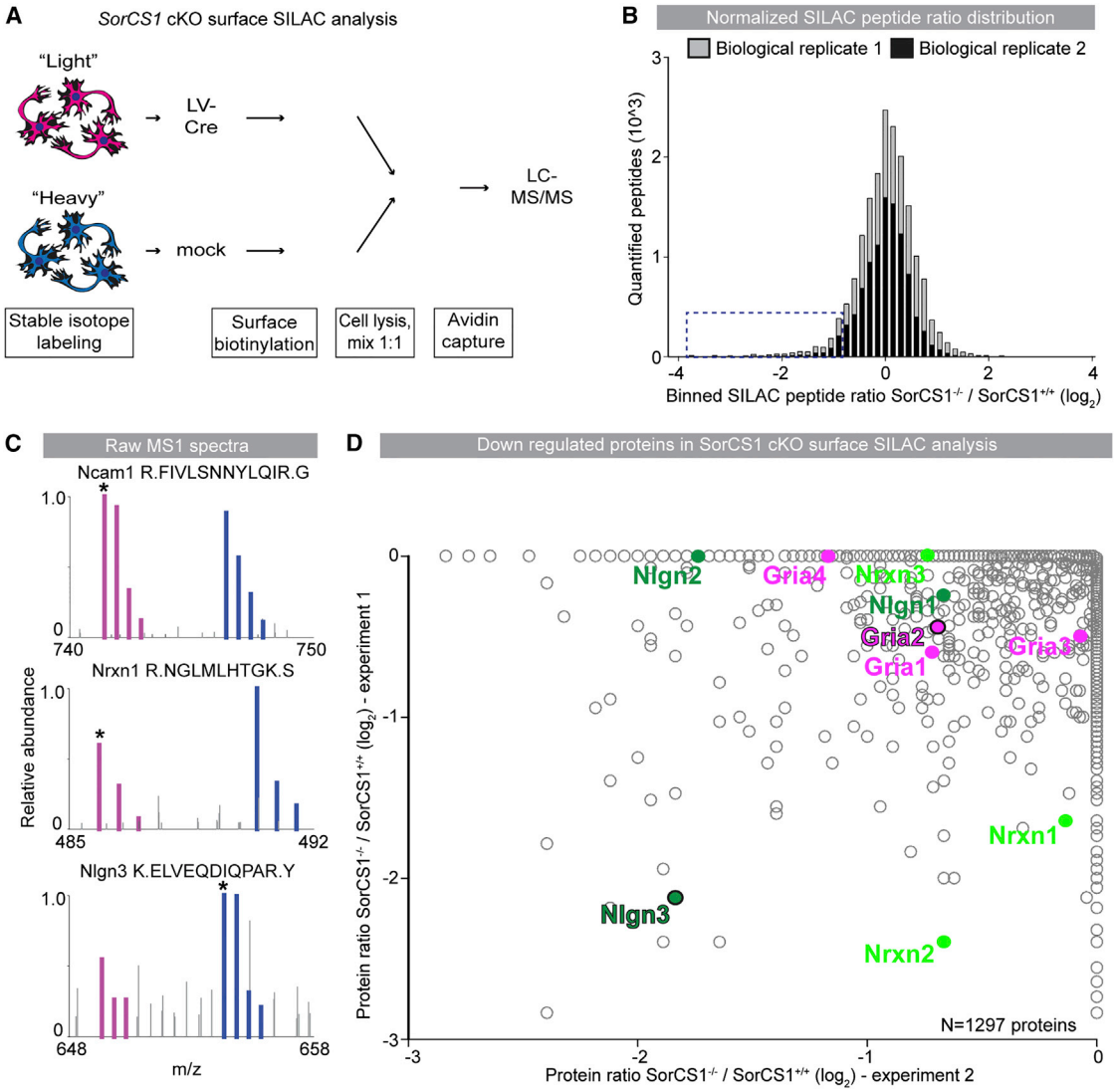

Figure 5. Quantitative Surface Proteome Analysis Reveals Reduced Surface Levels of Nrxn, Nlgn, and AMPARs in *SorCS1*-Deficient Neurons

(A) Experimental scheme *SorCS1* cKO surface SILAC analysis. Mock-infected *SorCS1*$^{flox/flox}$ neurons were grown in SILAC media (heavy, blue) and biotinylated surface proteins were isolated and quantified compared to LV-Cre-infected *SorCS1*$^{flox/flox}$ neurons (*SorCS1* cKO; light, red) using MS (see Supplemental Experimental Procedures).

(B) Corrected peptide ratio distributions for 2 independent biological replicates (experiment 1 and 2) show normal distributions with tails skewed toward peptides with a reduced SILAC ratio in the *SorCS1* cKO condition (dotted blue box).

(C) Raw MS1 scans for Nrxn1 and Nlgn3 show reduced intensity for *SorCS1* cKO condition (red) while Ncam1 is unchanged. Starred peaks were identified by MS/MS.

(D) Cross-hair scatter plot from two independent experiments shows that Nrxn1 and Nrxn2, Nlgn3, and Gria1 and Gria2 are among the most strongly downregulated proteins in *SorCS1*-deficient neurons. Proteins measured as downregulated in one experiment but unquantified in the other are shown on that axis as 0. Outlined proteins were determined as significantly downregulated (see Supplemental Experimental Procedures). Student's t test $p < 0.05$; n = 1,297 proteins. See also Figure S5.

a logarithmic scale, with the lowest ratios indicating the most strongly decreased proteins in *SorCS1*-deficient neurons. This global surface proteome analysis also identified Nrxn1 and Nrxn2 as among the proteins with the strongest decrease in surface expression after loss of *SorCS1* (Figure 5D; Table S4). The surface levels of Nlgn3 and the AMPAR subunit Gria2 (GluA2), proteins that were identified in the SorCS1 interactome analysis (Figure 4; Tables S2 and S3), were also decreased (Figure 5D). Additional receptors, such as APP and Plexin, from the SorCS1 interactome analysis showed reduced surface expression in *SorCS1* KO neurons (Table S4). Thus, multiple receptors, including the Nrxn and Nlgn synaptic adhesion molecules and AMPARs, depend on SorCS1 for normal surface expression. These results identify SorCS1 as a global regulator of receptor surface trafficking and indicate that loss of *SorCS1* alters surface proteome composition.

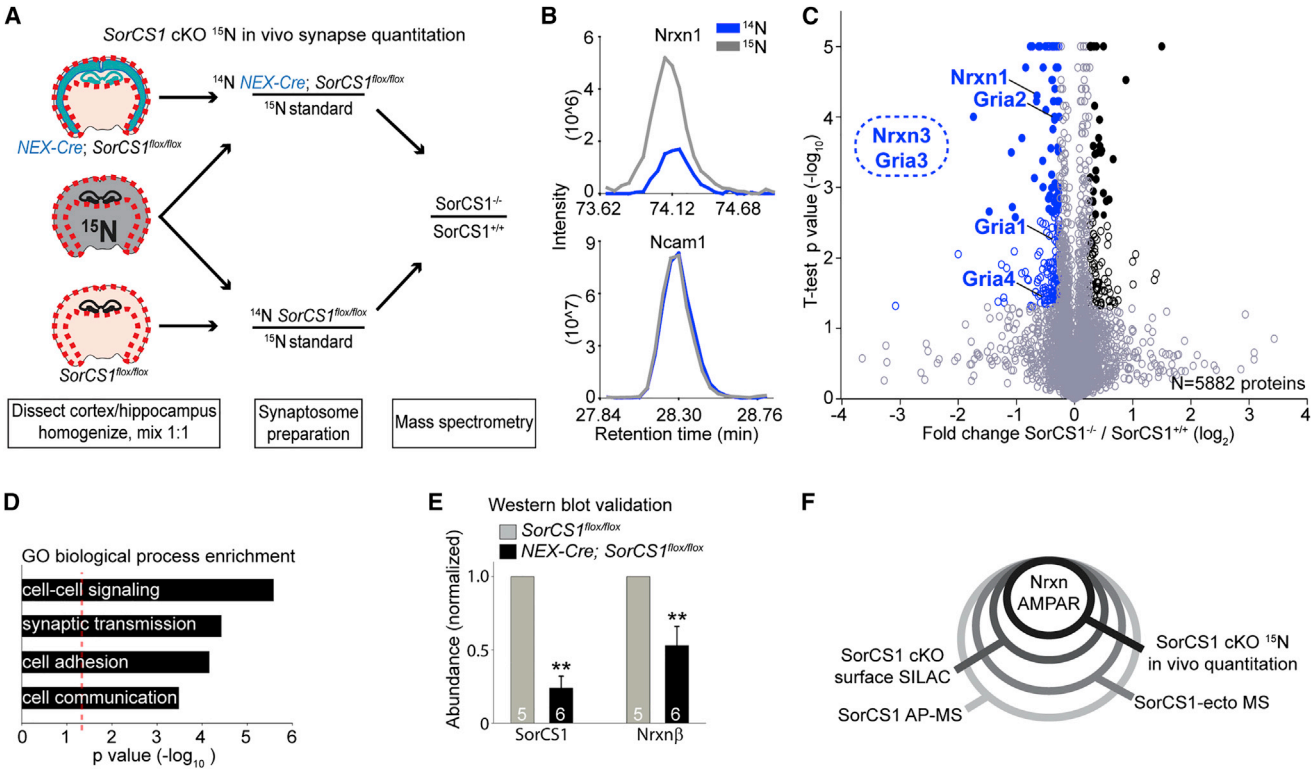

Figure 6. In Vivo Loss of *SorCS1* Decreases Synaptic Abundance of Adhesion and Glutamate Receptors

(A) Quantitative in vivo proteomic scheme to identify synaptic proteins regulated by SorCS1. *NEX-Cre:SorCS1*$^{flox/flox}$ (n = 6) or *SorCS1*$^{flox/flox}$ (n = 5) brain region homogenates were mixed 1:1 with ^{15}N internal standard. Synaptosomes were prepared simultaneously and analyzed by MS (see Experimental Procedures).

(B) MS1 reconstructed chromatograms of representative peptides. Elution profile MS1 traces are shown for a representative peptide from Nrxn and Ncam1. Internal standard ^{15}N signal in gray, *NEX-Cre:SorCS1*$^{flox/flox}$ ^{14}N signal in blue.

(C) Proteomic summary volcano plot, x axis = $\log_2$ *SorCS1*$^{-/-}$ / *SorCS1*$^{+/+}$, y axis = $-\log_{10}$ t test p value. N = 5,882 total proteins represented: 299 (5.1%) regulated proteins (p value $\leq$ 0.05 and $\geq$ 20% altered expression; blue and black open circles) and 104 most-confident proteins (Benjamini-Hochberg corrected p value $\leq$ 0.05 and $\geq$ 20% altered expression and $\leq$ 0.05; blue and black filled circles). p values = 0 were graphed as 0.00001. Nrxn3 and Gria3 were below the limit of detection in *SorCS1*$^{-/-}$ and were considered singletons (dotted oval).

(D) Panther GO biological process analysis of significantly downregulated proteins graphed in rank order by decreasing p value (154 of 191 downregulated proteins mapped, p value < 0.05). Dotted red line indicates significance cut-off (p < 0.05).

(E) Western blot validation of SorCS1 and Nrxnβ levels relative to β-tubulin in synaptosome extracts used in quantitative MS screen. **p < 0.005 by Student's t test. Bar graph shows mean ± STD; number in bars indicates *n* for each condition.

(F) Venn diagram. Four independent proteomics approaches significantly identify Nrxns and AMPARs as key proteins regulated by SorCS1 (See Supplemental Experimental Procedures for details). See also Figure S6.

In Vivo Loss of *SorCS1* Decreases Synaptic Abundance of Adhesion and Glutamate Receptors

Many of the receptors depending on SorCS1 for their surface expression are synaptic proteins. To determine whether SorCS1 regulates receptor abundance at synapses in vivo, we performed a quantitative analysis of synaptic proteomes from *SorCS1*$^{flox/flox}$ mice crossed with *NEX-Cre* transgenic mice to specifically decrease *SorCS1* expression in principal cortical and hippocampal neurons. Cortex and hippocampus were dissected from mature *NEX-Cre:SorCS1*$^{flox/flox}$ mice and *SorCS1*$^{flox/flox}$ control mice, homogenized, and mixed 1:1 with an internal standard consisting of cortex and hippocampus dissected from non-transgenic mice that were metabolically labeled in vivo with the stable isotope ^{15}N (Figure 6A; Supplemental Experimental Procedures). We then performed LC-MS/MS analysis of each ^{14}N biological replicate with the common ^{15}N internal standard simultaneously to obtain relative ^{14}N/^{15}N peptide ratios (*SorCS1* cKO ^{15}N in vivo synapse quantitation; Figures 6A, S6A, and S6B). We quantified a total of 5,882 proteins and found that 95% of the synaptic proteome was not significantly affected by loss of *SorCS1*. We identified 299 significantly regulated proteins (5.1% of total proteins; t test p value $\leq$ 0.05 and $\geq$ 20% change in expression), of which 191 were downregulated and 108 were upregulated (Table S5).

Manual inspection of the raw MS1 m/z spectra indicated downregulated levels of Nrxn1 in *NEX-Cre:SorCS1*$^{flox/flox}$ synaptosomes in comparison to those in ^{15}N controls, whereas the abundance of Ncam1 was not altered (Figures 6B and S6A). Overall, Nrxn1 was among the most significantly downregulated proteins in *SorCS1*-deficient synaptosomes (1.5-fold downregulation; Figures 6C, S6C, and S6D; Table S5). To verify the quantitative MS results, we analyzed Nrxn protein levels

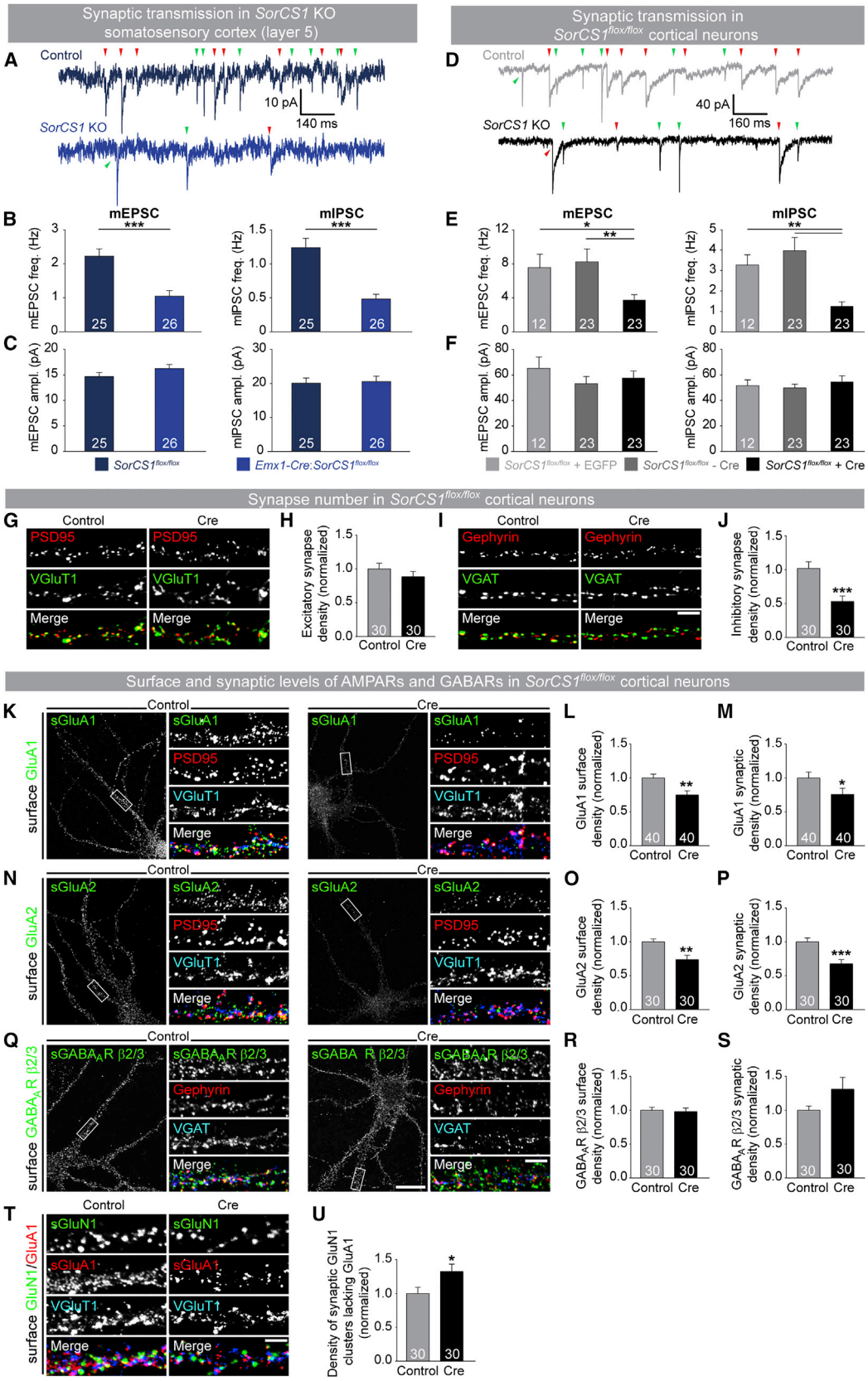

(legend on next page)

in *SorCS1*$^{flox/flox}$ and *NEX-Cre:SorCS1*$^{flox/flox}$ synaptosomes by western blot and found that loss of *SorCS1* significantly decreased Nrxn levels (Figures 6E and S6E).

In addition to Nrxn, several other synaptic adhesion molecules were detected among the significantly downregulated proteins in *NEX-Cre:SorCS1*$^{flox/flox}$ synaptosomes, including Contactin-4 (Cntn4; 2-fold downregulation) and leucine-rich repeat (LRR)-containing synaptic adhesion molecules such as LRRC4B (NGL-3; 1.5-fold downregulation). Ionotropic glutamate receptor abundance was also significantly decreased in *SorCS1* KO synaptosomes. All four AMPAR subunits, Gria1–Gria4 (GluA1–GluA4), and the NMDA receptor subunits Grin2a (GluN2A) and Grin2b (GluN2B) were downregulated (all 1.2-fold downregulation; Figures 6C and S6D; Table S5). Taken together, manual inspection of downregulated proteins suggests that loss of *SorCS1* decreases the abundance of adhesion proteins and glutamate receptors.

We next performed Gene Ontology (GO) analysis to identify over-represented biological processes and classes of proteins in our dataset in an unbiased way. We compared the significantly downregulated proteins to the total collection of quantified proteins and found that cell-cell signaling, synaptic transmission, cell adhesion, and cell communication were the four most significantly over-represented biological processes (Figures 6D, S6F, and S6H). In contrast, GO analysis of upregulated proteins did not reveal such significant enrichment of any process (Figure S6G). Grouping of significantly altered proteins by protein class showed that receptors and ion channels together represented roughly half of all downregulated proteins (Figure S6I). Thus, loss of *SorCS1* in principal glutamatergic neurons of the hippocampus and cortex decreases the synaptic abundance of receptors regulating cell adhesion and synaptic transmission in vivo.

Importantly, Nrxns and AMPARs were detected in four different, unbiased proteomic approaches assessing SorCS1 function (Figure 6F): SorCS1-ecto MS and AP-MS (Figure 4), *SorCS1* cKO surface SILAC analysis (Figure 5), and *SorCS1* cKO ^{15}N in vivo synapse quantitation (Figure 6). Specifically, Gria2 (GluA2) was significantly identified with all four approaches (joint probability of such event occurring by chance = 0.0009; see Supplemental Experimental Procedures). In addition, three more proteins were significantly detected using three of these methods: these proteins were Nrxn1 (*SorCS1* cKO ^{15}N in vivo synapse quantitation, *SorCS1* cKO surface SILAC, and SorCS1-ecto MS; joint probability = 0.0023), Nrxn2 (*SorCS1* cKO surface SILAC, SorCS1-ecto MS, and SorCS1 AP-MS; joint probability = 0.0107), and Gria3 (GluA3) (*SorCS1* cKO ^{15}N in vivo synapse quantitation, *SorCS1* cKO surface SILAC, and SorCS1 AP-MS; joint probability = 0.0015). Together, the combined results from four different approaches indicate that Nrxns and AMPARs represent key proteins depending on SorCS1 for their surface and synaptic abundance.

SorCS1 Is Required for Basal Glutamatergic and GABAergic Synaptic Transmission

In the final series of experiments, we asked how an altered abundance of synaptic receptors in the absence of *SorCS1* affects synaptic transmission. We recorded spontaneous miniature excitatory and inhibitory postsynaptic currents (mEPSCs and mIPSCs, respectively) from somatosensory layer 5 pyramidal neurons in P18-21 acute cortical slices from control *SorCS1*$^{flox/flox}$ and *Emx1-Cre:SorCS1*$^{flox/flox}$ mice to assess basal synaptic transmission. The frequency of mEPSCs and mIPSCs was strongly decreased in *Emx1-Cre:SorCS1*$^{flox/flox}$ cortical neurons in comparison to that in controls, whereas amplitude and decay time were not affected (Figures 7A–7C and S7A–S7C). We next cultured *SorCS1*$^{flox/flox}$ cortical neurons and electroporated them with Cre or GFP control plasmids. We recorded mEPSCs and mIPSCs from DIV12–DIV16 neurons and

Figure 7. SorCS1 Is Required for Basal Glutamatergic and GABAergic Synaptic Transmission

(A–C) Analysis of synaptic transmission in layer 5 somatosensory cortical neurons in *SorCS1*$^{flox/flox}$ (control) and *Emx1-Cre:SorCS1*$^{flox/flox}$ (*SorCS1* KO) acute slices.

(A) Example traces. Segregation of mEPSCs (green arrowheads) and mIPSCs (red arrowheads) was based on difference in decay time kinetics.

(B and C) mEPSC and mIPSC frequency, but not amplitude, are decreased in *SorCS1* KO layer 5 neurons. ***$p < 0.001$ by Mann-Whitney test.

(D–F) Analysis of synaptic transmission in *SorCS1*$^{flox/flox}$ dissociated cortical neurons electroporated with EGFP (control) or Cre (*SorCS1* KO).

(D) Example traces.

(E and F) Reduced mEPSC and mIPSC frequency, but not amplitude, in *SorCS1*$^{flox/flox}$ neurons expressing Cre (+Cre) compared to neighboring non-electroporated neurons (−Cre) or control neurons (+EGFP). *$p < 0.05$, **$p < 0.01$ by Kruskal-Wallis test followed by Dunn's post hoc test.

(G–J) Analysis of synapse density in *SorCS1*$^{flox/flox}$ cortical neurons.

(G and H) VGluT1- and PSD95-positive puncta density is not changed in DIV14 *SorCS1*$^{flox/flox}$ cortical neurons electroporated with Cre in comparison to EGFP-electroporated cells (control).

(I and J) Decreased density of Gephyrin- and VGAT-positive puncta in *SorCS1* KO neurons.

(J) ***$p < 0.001$ Mann-Whitney test.

(K–U) Analysis of AMPAR and $GABA_AR$ surface and synaptic expression in *SorCS1*$^{flox/flox}$ cortical neurons.

(K) *SorCS1*$^{flox/flox}$ cortical neurons electroporated with EGFP (control) or Cre (Cre) plasmids were immunostained on DIV14 for surface GluA1 under non-permeabilizing conditions. After permeabilization, neurons were stained for GFP, PSD95, and VGluT1.

(L) Decreased GluA1 surface expression in *SorCS1* KO neurons.

(M) Decreased synaptic surface levels of GluA1 in *SorCS1* KO neurons.

(N–P) Decreased cell surface and synaptic GluA2 levels in *SorCS1* KO neurons.

(Q) Surface $GABA_AR$ β2/3 staining in *SorCS1*$^{flox/flox}$ cortical neurons.

(R–S) $GABA_AR$ β2/3 surface (R) and synaptic (S) expression are not affected in *SorCS1* KO neurons. *$p < 0.05$, **$p < 0.01$ and ***$p < 0.001$ Mann-Whitney test.

(T) DIV14 *SorCS1*$^{flox/flox}$ cortical neurons electroporated with EGFP (control) and Cre (Cre) surface-labeled for GluN1 and GluA1.

(U) Quantification of the density of synaptic surface GluN1 clusters lacking surface GluA1 normalized to controls. *$p < 0.05$ by Mann-Whitney test. Bar graphs show mean ± SEM; number in bars indicates number of cells analyzed for each condition in three–four independent experiments. Scale bars in (G), (I), (K), (N), (Q), and (T), 5 μm; whole cell panels in (K), (N), and (Q), 20 μm. See also Figure S7.

found a similar decrease in the frequency of these events in *SorCS1*$^{flox/flox}$ neurons expressing Cre (+ Cre) in comparison to that in control *SorCS1*$^{flox/flox}$ neurons (+ EGFP) (Figures 7D and 7E). Amplitude, decay time, and membrane potential were not affected by loss of *SorCS1* (Figures 7F and S7D–S7G). To test whether the effects of loss of *SorCS1* on spontaneous synaptic transmission are cell-autonomous, we recorded mPSCs from neighboring non-electroporated *SorCS1*$^{flox/flox}$ neurons (−Cre) in Cre-electroporated cultures. We found no change in the frequency, amplitude, or decay kinetics of mEPSCs and mIPSCs in −Cre *SorCS1*$^{flox/flox}$ neurons (Figures 7E and 7F and S7D–S7G), indicating that the effects of loss of *SorCS1* on mPSC frequency are cell-autonomous. Together, these results show that the tone of spontaneous glutamatergic and GABAergic transmission is reduced in the absence of *SorCS1*.

A decrease in mPSC frequency could be due to a reduced probability of spontaneous release or a decrease in synapse density. Given that our data indicates that the decrease in mPSC frequency occurs only in *SorCS1*-deficient neurons and not in neighboring non-electroporated cells, we focused on postsynaptic mechanisms. We quantified excitatory and inhibitory synapse density in DIV14 *SorCS1*$^{flox/flox}$ cortical neurons electroporated with Cre or control plasmids. Loss of *SorCS1* did not affect the density of puncta positive for the excitatory synaptic markers PSD95 and VGluT1 (Figures 7G and 7H), nor did it affect the density of dendritic protrusions (control 0.432 ± 0.045 versus Cre 0.445 ± 0.039 protrusions/μm; mean ± SEM; n = 10 neurons per condition; not significant by Mann-Whitney test). *SorCS1* KO neurons displayed a significant decrease in the density of puncta positive for the inhibitory synaptic markers Gephyrin and VGAT (Figures 7I and 7J). These effects were specific to cortical neurons, given that loss of *SorCS1* in hippocampal neurons did not affect synapse density or mEPSC frequency (Figures S7H–S7N). However, SorCS1 overexpression in hippocampal neurons increased functional excitatory synapse density but did not affect inhibitory synapse density (Figures S7O–S7V). These results show that loss of *SorCS1* differentially affects excitatory and inhibitory synapses: excitatory synapse density is unaltered in *SorCS1* KO neurons, whereas inhibitory synapse density is decreased.

The decreased inhibitory synapse density in *SorCS1* KO neurons can account for the reduced mIPSC frequency in these cells, but the decrease in mEPSC frequency must be due to another mechanism. Given that AMPARs were consistently identified as regulated by SorCS1 (Figure 6F), we asked whether a loss of AMPAR surface expression at synapses might explain the decreased mEPSC frequency in *SorCS1* KO neurons. Cortical DIV14 *SorCS1*$^{flox/flox}$ neurons electroporated with Cre or GFP were fixed and immunostained under non-permeabilizing conditions for surface GluA1- and GluA2-containing AMPARs. We found a significant decrease in overall GluA1 and GluA2 surface levels (Figure 7K,L, N, O), as well as synaptic GluA1 and GluA2 levels, in *SorCS1* KO neurons compared to control cells (Figure 7K, M, N, P). In contrast, dendritic and synaptic surface levels of the β2/3 subunit of the inhibitory $GABA_A$ receptor were not altered in *SorCS1* KO neurons (Figure 7Q-S). These results indicate that SorCS1 is required to maintain surface and synaptic abundance of AMPARs.

The decreased mEPSC frequency in *SorCS1* KO neurons suggests that a population of synapses lacks AMPAR surface expression in the absence of *SorCS1*. To test whether the fraction of AMPAR-lacking synapses is increased in *SorCS1* KO neurons, we labeled surface GluA1 and the NMDA-receptor-subunit GluN1 under non-permeabilizing conditions, followed by a permeabilization step to label VGluT1 (Figure 7T). Quantification of the density of synaptic surface GluN1 puncta lacking surface GluA1 expression revealed a significant increase in the fraction of AMPAR-lacking synapses in *SorCS1* KO neurons (Figure 7U). Together, these results show that loss of *SorCS1* differentially affects excitatory and inhibitory synapses: excitatory synapse density is unaffected in *SorCS1* KO neurons, but the fraction of synapses lacking functional AMPARs is increased. The density of inhibitory synapses, on the other hand, is decreased in *SorCS1* KO neurons, but $GABA_AR$ surface expression at remaining inhibitory synapses is not impaired.

DISCUSSION

Here, we identify the sorting receptor SorCS1 as a key regulator of synaptic receptor trafficking. Our proteomic analyses identify the synaptic adhesion molecule Nrxn and the AMPA glutamate receptor as the major proteins sorted by SorCS1. SorCS1 localizes to early and recycling endosomes and regulates Nrxn and AMPAR surface expression in neurons. SorCS1 is found in a molecular complex with Nrxn, other synaptic adhesion molecules, and AMPARs. In cultured neurons, SorCS1 maintains surface levels of these receptors. In vivo, SorCS1 maintains the synaptic abundance of receptors regulating cell adhesion and synaptic transmission, including Nrxns and AMPARs. Loss of *SorCS1* decreases both glutamatergic and GABAergic synaptic transmission as a result of impaired AMPAR surface levels at excitatory synapses and a decrease in inhibitory synapse density, respectively. Together, our results show that SorCS1 regulates the trafficking of neuronal receptors that are essential for synaptic function.

Regulation of Synaptic Receptor Trafficking by SorCS1

Our findings show that the surface and synaptic levels of multiple receptors are affected in the absence of SorCS1. How can the loss of a sorting protein affect the expression of many surface receptors? Our MS analysis of affinity-purified SorCS1 complexes identified AP-2-complex subunits. The AP-2 complex plays an important role in the sorting of receptors from the cell surface to endosomes (Traub, 2009), which regulate many processes in neurons, including the cell surface distribution of receptors (Yap and Winckler, 2012). In addition to the AP-2 complex, SorCS1 also interacts with the retromer protein Vps35 (Lane et al., 2010; Lane et al., 2013). The retromer complex is emerging as a major regulator of endosomal sorting (Burd and Cullen, 2014) and regulates retrieval of transmembrane proteins from endosomes to the TGN for recycling (Bonifacino and Hurley, 2008), as well as surface delivery of receptors from endosomes (Small and Petsko, 2015). Knockdown of Vps35 in HeLa cells downregulates the surface expression of 152 membrane proteins (Steinberg et al., 2013). In these cells, the retromer maintains surface expression and prevents lysosomal degradation

of a broad array of receptors. The changes in surface proteome composition after Vps35 knockdown in HeLa cells are reminiscent of the changes in receptor surface expression we observe in *SorCS1* KO neurons. By interacting with the AP-2 and retromer complexes, SorCS1 links to major intracellular sorting pathways regulating endocytosis and recycling of cargo, thereby acting as a hub in the control of receptor surface expression in neurons. In addition to direct effects of SorCS1 on receptor trafficking, some of the changes in protein levels after *SorCS1* loss of function are most likely indirect. These might represent proteins that depend on downregulated receptors for their stabilization or represent compensatory changes.

Four independent proteomic approaches identified Nrxn and AMPARs as the major proteins sorted by SorCS1, and two independent quantitative proteomic analyses indicated that their surface and synaptic levels were decreased in *SorCS1* KO neurons. Our data show that in the absence of SorCS1-mediated sorting, Nrxn accumulates on the dendritic surface and is lost from the axonal surface. A lack of suitable antibodies for the detection of endogenous SorCS1 and Nrxn forced us to rely on overexpression of tagged constructs to address Nrxn trafficking, which is a limitation of our study. The exact localization of Nrxns, and whether Nrxns may also have a function in dendrites, remains unclear. Loss of α-Nrxns affects NMDAR function and dendritic morphology (Dudanova et al., 2007; Kattenstroth et al., 2004), but conflicting results have been reported on the effects of dendritic overexpression of Nrxn on synapse density (Taniguchi et al., 2007; Zhang et al., 2010). Regardless of a postsynaptic function of Nrxn, our results suggest that somatodendritic sorting is required to maintain Nrxn levels on the axon surface. Interestingly, the axonal targeting of the receptors L1/NgCAM and the Nrxn family member CASPR2 depends on endocytosis in the somatodendritic compartment. Upon interference with endocytosis, these proteins are mis-sorted to the somatodendritic surface and degraded in lysosomes (Bel et al., 2009; Yap et al., 2008). Similarly, axonal trafficking of Nrxn may depend on SorCS1-mediated endocytosis and endosomal sorting in the somatodendritic domain, followed by transport of Nrxn into axons. In conclusion, our data suggests that SorCS1 mediates sorting of cargo proteins in endosomes to regulate their recycling back to the cell surface and prevent cargo from entering lysosomal degradation pathways. More work is needed to delineate the exact mechanisms by which SorCS1 regulates these intracellular trafficking pathways.

SorCS1 and Synaptic Function

Loss of *SorCS1* reduced spontaneous glutamatergic and GABAergic synaptic transmission. The decrease in mPSC frequency in *SorCS1* KO neurons is cell-autonomous and did not occur in neighboring non-transfected cells, indicating a postsynaptic origin of these defects. We do not exclude the possibility that there may be additional presynaptic defects in *SorCS1* KO neurons that we were unable to resolve in our current experiments. Several proteins regulating presynaptic function are downregulated in *SorCS1* KO synaptosomes (Table S5), but these do not seem to be involved in the phenotype we observe here. Instead, the decreased glutamatergic transmission in *SorCS1* KO neurons could be attributed to impaired surface expression of AMPARs. Our data indicate an increased fraction of excitatory synapses lacking functional AMPARs in *SorCS1* KO neurons, whereas the remaining synapses appear to have normal AMPAR content. Similar impairments in AMPAR surface levels have been observed after loss of the intracellular trafficking regulators Vps35, the sorting nexin SNX27, and Neurobeachin (Choy et al., 2014; Hussain et al., 2014; Loo et al., 2014; Nair et al., 2013; Wang et al., 2013). SorCS1, Vps35, and SNX27 are all linked to retromer function, highlighting the importance of this complex in regulating AMPAR trafficking.

Impaired trafficking of synaptic adhesion molecules could also contribute to the decreased AMPAR synaptic levels in *SorCS1*-deficient neurons. The interaction of Nrxn with Nlgn1 and LRRTM2 controls AMPAR trafficking (Aoto et al., 2013). Nlgn3, which was strongly downregulated on the surface of *SorCS1* KO neurons, also affects AMPAR trafficking (Chanda et al., 2015). Thus, mis-sorting of adhesion molecules in *SorCS1* KO neurons could affect AMPAR trafficking. The decreased inhibitory synaptic transmission in *SorCS1* KO neurons, on the other hand, did not result from impaired $GABA_AR$ trafficking but could be attributed to a decrease in inhibitory synapse density. Decreased abundance of Nlgn2 (Table S5) and Nlgn3 (Figure 5), which localize to inhibitory synapses (Budreck and Scheiffele, 2007; Poulopoulos et al., 2009), could lead to reductions in inhibitory synapse density. Alternatively, this decrease might reflect a compensatory response to the reduced glutamatergic transmission in *SorCS1* KO neurons, given that overexpression of SorCS1 in hippocampal neurons did not affect inhibitory synapse density.

SorCS1 and Synaptopathies

SORCS genes have been associated with a range of synaptopathies, including Alzheimer disease and autism (Christoforou et al., 2011; Grupe et al., 2006; Lionel et al., 2011; Ollila et al., 2009; Reitz et al., 2011; Sanders et al., 2012). Impaired receptor trafficking resulting from *SORCS1* mutations could contribute to synaptic-composition and -function defects underlying synaptopathies. A SorCS1 cargo protein directly relevant to disease is APP, which accumulates in endosomes in the absence of SorCS1, increasing levels of Alzheimer Aβ peptide (Lane et al., 2010; Lane et al., 2013; Reitz et al., 2011), which is detrimental to synapses (Mucke and Selkoe, 2012). Loss of *SorCS1* also affects trafficking of the adhesion proteins Nlgns and Nrxns, which regulate many aspects of synapse development and function (Krueger et al., 2012) and have been linked to autism and schizophrenia (Südhof, 2008). Interestingly, SorCS2 acts as a coreceptor of the p75 neurotrophin receptor in mediating proneurotrophin-induced growth cone collapse (Anastasia et al., 2013; Deinhardt et al., 2011; Glerup et al., 2014), suggesting that other SorCS proteins could affect neuronal wiring in different ways.

Our functional analysis indicates that the impact of loss of *SorCS1* on excitatory synapses is relatively subtle, increasing the fraction of functional AMPAR-lacking synapses, thereby dampening synaptic transmission but not abolishing it. The persistence of immature, AMPAR-lacking synapses could affect the plasticity and activity-dependent postnatal refinement of cortical

circuits, and has been observed in a model of fragile X syndrome (Harlow et al., 2010). Reduced synaptic activity might eventually lead to synapse loss and neuronal degeneration. Impaired intracellular trafficking is emerging as a common theme in neurodegenerative diseases (Small and Petsko, 2015), underscoring the importance of regulation of receptor trafficking for the maintenance of synaptic composition and function.

EXPERIMENTAL PROCEDURES

Additional details are provided in online Supplemental Experimental Procedures.

Neuronal Cultures and Transfections

Neurons were cultured from E18 or P0/1 Long-Evans rats (Charles River) or P1 C57BL/6J SorCS1$^{flox/flox}$ mice and plated on poly-D-lysine (Millipore) and laminin (Invitrogen) coated glass coverslips (Glaswarenfabrik Karl Hecht), chamber slides, and dishes (Nalge Nunc International). Neurons were maintained in Neurobasal-A medium or Neurobasal medium (Invitrogen) supplemented with B27, glucose, glutamax, penicillin/streptomycin (Invitrogen), 20 μg/ml insulin (Sigma), and 25 μM β-mercaptoethanol. Neurons were electroporated with plasmid DNA just before plating with an AMAXA Nucleofector kit (Lonza). Transfections were performed at 7 days in vitro with Effectene (QIAGEN).

Animal Experiments

All animal experiments were conducted according to the University of California, San Diego (UCSD), The Scripps Research Institute (TSRI), and Katholieke Universiteit (KU) Leuven ethical guidelines and approved by the UCSD institutional animal care and use committee (IACUC; approved protocol nos. S03154 and S03155), TSRI IACUC and Department of Animal Resources (approved protocol no. 07-0083), and the KU Leuven ethical committee (approved protocol nos. P015-2013 and P026-2013). For euthanasia, newborn pups were immediately decapitated, and adult animals were injected with a lethal dose of sodium pentobarbital.

SUPPLEMENTAL INFORMATION

Supplemental Information includes Supplemental Experimental Procedures, seven figures, and five tables and can be found with this article online at http://dx.doi.org/10.1016/j.neuron.2015.08.007.

AUTHOR CONTRIBUTIONS

J.N.S, L.F.R, K.D.W, J.R.Y, A.G, and J.d.W. designed research; J.N.S., L.F.R, K.D.W., J.d.W., R.W., L.A.D-W., H.R., I.C., Y.W., R.Z., M.L., K.M.V., M.O.S., J.K.A., and E.A.H performed research; J.N.S., L.F.R., M.L., K.M.V., J.K.A., O.T., A.D.A., J.R.Y., and J.d.W. contributed new reagents/analytical tools; J.N.S., L.F.R., K.D.W., R.W., H.R., I.C., Y.W., R.Z., M.L., and J.d.W analyzed data; and J.N.S. and J.d.W. wrote the paper.

ACKNOWLEDGMENTS

We thank Patrik Verstreken, Rose Goodchild, Matthew Holt, Bassem Hassan, Kevin Lűthy, Christopher Parkhurst, and Peter Penzes for comments on the manuscript; Casper Hoogenraad, Wim Annaert, and Ragna Sannerud for reagents and advice; Davide Comoletti for providing Nrxn-ecto-Fc stable cell lines; and Sung Kyu Park, Merve Oney, Christine Wu, Mohit Patel, Margaret Butko, Jacqueline Benthuysen, and Max Caccese for technical assistance. This work was supported by NIH awards F32AG039127 and 4 R00DC013805-02 (J.N.S.); Marie Sklodowska-Curie postdoctoral fellowship H2020-MSCA-IF-2014 (L.F.R.); a postdoctoral fellowship from Fonds de Recherche du Québec – Nature et Technologies (M.L.A.); Conseil Régional Aquitaine (I.C. and O.T.); Fondation pour la Recherche Médicale and Agence Nationale de la Recherche (O.T.); NIH grants R01MH068578 and R01NS067216 (A.G.); NIH grants P41 GM103533 and R01 MH067880 (J.R.Y.); and a NARSAD Young Investigator Award from the Brain and Behavior Research Foundation, a European Research Council Starting Grant (311083), and a FWO Odysseus Grant (J.d.W.). The .raw files, search and quantitative results, and complete parameter files for all MS experiments are publicly available at http://fields.scripps.edu/published/SorCS_NRXN/.

Received: June 21, 2014
Revised: June 16, 2015
Accepted: August 3, 2015
Published: August 19, 2015

REFERENCES

Anastasia, A., Deinhardt, K., Chao, M.V., Will, N.E., Irmady, K., Lee, F.S., Hempstead, B.L., and Bracken, C. (2013). Val66Met polymorphism of BDNF alters prodomain structure to induce neuronal growth cone retraction. Nat. Commun. *4*, 2490.

Aoto, J., Martinelli, D.C., Malenka, R.C., Tabuchi, K., and Südhof, T.C. (2013). Presynaptic neurexin-3 alternative splicing trans-synaptically controls postsynaptic AMPA receptor trafficking. Cell *154*, 75–88.

Bayés, A., Collins, M.O., Croning, M.D., van de Lagemaat, L.N., Choudhary, J.S., and Grant, S.G. (2012). Comparative study of human and mouse postsynaptic proteomes finds high compositional conservation and abundance differences for key synaptic proteins. PLoS ONE *7*, e46683.

Bel, C., Oguievetskaia, K., Pitaval, C., Goutebroze, L., and Faivre-Sarrailh, C. (2009). Axonal targeting of Caspr2 in hippocampal neurons via selective somatodendritic endocytosis. J. Cell Sci. *122*, 3403–3413.

Berninghausen, O., Rahman, M.A., Silva, J.P., Davletov, B., Hopkins, C., and Ushkaryov, Y.A. (2007). Neurexin Ibeta and neuroligin are localized on opposite membranes in mature central synapses. J. Neurochem. *103*, 1855–1863.

Bonifacino, J.S., and Hurley, J.H. (2008). Retromer. Curr. Opin. Cell Biol. *20*, 427–436.

Boucard, A.A., Chubykin, A.A., Comoletti, D., Taylor, P., and Südhof, T.C. (2005). A splice code for trans-synaptic cell adhesion mediated by binding of neuroligin 1 to alpha- and beta-neurexins. Neuron *48*, 229–236.

Breiderhoff, T., Christiansen, G.B., Pallesen, L.T., Vaegter, C., Nykjaer, A., Holm, M.M., Glerup, S., and Willnow, T.E. (2013). Sortilin-related receptor SORCS3 is a postsynaptic modulator of synaptic depression and fear extinction. PLoS ONE *8*, e75006.

Budreck, E.C., and Scheiffele, P. (2007). Neuroligin-3 is a neuronal adhesion protein at GABAergic and glutamatergic synapses. Eur. J. Neurosci. *26*, 1738–1748.

Burd, C., and Cullen, P.J. (2014). Retromer: a master conductor of endosome sorting. Cold Spring Harb. Perspect. Biol. *6*.

Cajigas, I.J., Will, T., and Schuman, E.M. (2010). Protein homeostasis and synaptic plasticity. EMBO J. *29*, 2746–2752.

Chanda, S., Aoto, J., Lee, S.J., Wernig, M., and Südhof, T.C. (2015). Pathogenic mechanism of an autism-associated neuroligin mutation involves altered AMPA-receptor trafficking. Mol. Psychiatry. Published online March 17, 2015. http://dx.doi.org/10.1038/mp.2015.20.

Choquet, D., and Triller, A. (2013). The dynamic synapse. Neuron *80*, 691–703.

Choy, R.W., Park, M., Temkin, P., Herring, B.E., Marley, A., Nicoll, R.A., and von Zastrow, M. (2014). Retromer mediates a discrete route of local membrane delivery to dendrites. Neuron *82*, 55–62.

Christoforou, A., McGhee, K.A., Morris, S.W., Thomson, P.A., Anderson, S., McLean, A., Torrance, H.S., Le Hellard, S., Pickard, B.S., StClair, D., et al. (2011). Convergence of linkage, association and GWAS findings for a candidate region for bipolar disorder and schizophrenia on chromosome 4p. Mol. Psychiatry *16*, 240–242.

de Wit, J., Sylwestrak, E., O'Sullivan, M.L., Otto, S., Tiglio, K., Savas, J.N., Yates, J.R., 3rd, Comoletti, D., Taylor, P., and Ghosh, A. (2009). LRRTM2 interacts with Neurexin1 and regulates excitatory synapse formation. Neuron *64*, 799–806.

Dean, C., Scholl, F.G., Choih, J., DeMaria, S., Berger, J., Isacoff, E., and Scheiffele, P. (2003). Neurexin mediates the assembly of presynaptic terminals. Nat. Neurosci. *6*, 708–716.

Deinhardt, K., Kim, T., Spellman, D.S., Mains, R.E., Eipper, B.A., Neubert, T.A., Chao, M.V., and Hempstead, B.L. (2011). Neuronal growth cone retraction relies on proneurotrophin receptor signaling through Rac. Sci. Signal. *4*, ra82.

Dudanova, I., Tabuchi, K., Rohlmann, A., Südhof, T.C., and Missler, M. (2007). Deletion of alpha-neurexins does not cause a major impairment of axonal pathfinding or synapse formation. J. Comp. Neurol. *502*, 261–274.

Fairless, R., Masius, H., Rohlmann, A., Heupel, K., Ahmad, M., Reissner, C., Dresbach, T., and Missler, M. (2008). Polarized targeting of neurexins to synapses is regulated by their C-terminal sequences. J. Neurosci. *28*, 12969–12981.

Farías, G.G., Cuitino, L., Guo, X., Ren, X., Jarnik, M., Mattera, R., and Bonifacino, J.S. (2012). Signal-mediated, AP-1/clathrin-dependent sorting of transmembrane receptors to the somatodendritic domain of hippocampal neurons. Neuron *75*, 810–823.

Giagtzoglou, N., Ly, C.V., and Bellen, H.J. (2009). Cell adhesion, the backbone of the synapse: "vertebrate" and "invertebrate" perspectives. Cold Spring Harb. Perspect. Biol. *1*, a003079.

Glerup, S., Olsen, D., Vaegter, C.B., Gustafsen, C., Sjoegaard, S.S., Hermey, G., Kjolby, M., Molgaard, S., Ulrichsen, M., Boggild, S., et al. (2014). SorCS2 regulates dopaminergic wiring and is processed into an apoptotic two-chain receptor in peripheral glia. Neuron *82*, 1074–1087.

Graf, E.R., Zhang, X., Jin, S.X., Linhoff, M.W., and Craig, A.M. (2004). Neurexins induce differentiation of GABA and glutamate postsynaptic specializations via neuroligins. Cell *119*, 1013–1026.

Grant, S.G. (2012). Synaptopathies: diseases of the synaptome. Curr. Opin. Neurobiol. *22*, 522–529.

Grupe, A., Li, Y., Rowland, C., Nowotny, P., Hinrichs, A.L., Smemo, S., Kauwe, J.S., Maxwell, T.J., Cherny, S., Doil, L., et al. (2006). A scan of chromosome 10 identifies a novel locus showing strong association with late-onset Alzheimer disease. Am. J. Hum. Genet. *78*, 78–88.

Harlow, E.G., Till, S.M., Russell, T.A., Wijetunge, L.S., Kind, P., and Contractor, A. (2010). Critical period plasticity is disrupted in the barrel cortex of FMR1 knockout mice. Neuron *65*, 385–398.

Hermey, G. (2009). The Vps10p-domain receptor family. Cell. Mol. Life Sci. *66*, 2677–2689.

Hermey, G., Riedel, I.B., Rezgaoui, M., Westergaard, U.B., Schaller, C., and Hermans-Borgmeyer, I. (2001). SorCS1, a member of the novel sorting receptor family, is localized in somata and dendrites of neurons throughout the murine brain. Neurosci. Lett. *313*, 83–87.

Hermey, G., Plath, N., Hübner, C.A., Kuhl, D., Schaller, H.C., and Hermans-Borgmeyer, I. (2004). The three sorCS genes are differentially expressed and regulated by synaptic activity. J. Neurochem. *88*, 1470–1476.

Hussain, N.K., Diering, G.H., Sole, J., Anggono, V., and Huganir, R.L. (2014). Sorting Nexin 27 regulates basal and activity-dependent trafficking of AMPARs. Proc. Natl. Acad. Sci. USA *111*, 11840–11845.

Ichtchenko, K., Hata, Y., Nguyen, T., Ullrich, B., Missler, M., Moomaw, C., and Südhof, T.C. (1995). Neuroligin 1: a splice site-specific ligand for beta-neurexins. Cell *81*, 435–443.

Kattenstroth, G., Tantalaki, E., Südhof, T.C., Gottmann, K., and Missler, M. (2004). Postsynaptic N-methyl-D-aspartate receptor function requires alpha-neurexins. Proc. Natl. Acad. Sci. USA *101*, 2607–2612.

Ko, J., Fuccillo, M.V., Malenka, R.C., and Südhof, T.C. (2009). LRRTM2 functions as a neurexin ligand in promoting excitatory synapse formation. Neuron *64*, 791–798.

Krueger, D.D., Tuffy, L.P., Papadopoulos, T., and Brose, N. (2012). The role of neurexins and neuroligins in the formation, maturation, and function of vertebrate synapses. Curr. Opin. Neurobiol. *22*, 412–422.

Lane, R.F., Raines, S.M., Steele, J.W., Ehrlich, M.E., Lah, J.A., Small, S.A., Tanzi, R.E., Attie, A.D., and Gandy, S. (2010). Diabetes-associated SorCS1 regulates Alzheimer's amyloid-beta metabolism: evidence for involvement of SorL1 and the retromer complex. J. Neurosci. *30*, 13110–13115.

Lane, R.F., Steele, J.W., Cai, D., Ehrlich, M.E., Attie, A.D., and Gandy, S. (2013). Protein sorting motifs in the cytoplasmic tail of SorCS1 control generation of Alzheimer's amyloid-β peptide. J. Neurosci. *33*, 7099–7107.

Lionel, A.C., Crosbie, J., Barbosa, N., Goodale, T., Thiruvahindrapuram, B., Rickaby, J., Gazzellone, M., Carson, A.R., Howe, J.L., Wang, Z., et al. (2011). Rare copy number variation discovery and cross-disorder comparisons identify risk genes for ADHD. Sci. Transl. Med. *3*, 95ra75.

Loo, L.S., Tang, N., Al-Haddawi, M., Dawe, G.S., and Hong, W. (2014). A role for sorting nexin 27 in AMPA receptor trafficking. Nat. Commun. *5*, 3176.

Mucke, L., and Selkoe, D.J. (2012). Neurotoxicity of amyloid β-protein: synaptic and network dysfunction. Cold Spring Harb. Perspect. Med. *2*, a006338.

Nair, R., Lauks, J., Jung, S., Cooke, N.E., de Wit, H., Brose, N., Kilimann, M.W., Verhage, M., and Rhee, J. (2013). Neurobeachin regulates neurotransmitter receptor trafficking to synapses. J. Cell Biol. *200*, 61–80.

Nielsen, M.S., Madsen, P., Christensen, E.I., Nykjaer, A., Gliemann, J., Kasper, D., Pohlmann, R., and Petersen, C.M. (2001). The sortilin cytoplasmic tail conveys Golgi-endosome transport and binds the VHS domain of the GGA2 sorting protein. EMBO J. *20*, 2180–2190.

Nielsen, M.S., Gustafsen, C., Madsen, P., Nyengaard, J.R., Hermey, G., Bakke, O., Mari, M., Schu, P., Pohlmann, R., Dennes, A., and Petersen, C.M. (2007). Sorting by the cytoplasmic domain of the amyloid precursor protein binding receptor SorLA. Mol. Cell. Biol. *27*, 6842–6851.

Nielsen, M.S., Keat, S.J., Hamati, J.W., Madsen, P., Gutzmann, J.J., Engelsberg, A., Pedersen, K.M., Gustafsen, C., Nykjaer, A., Gliemann, J., et al. (2008). Different motifs regulate trafficking of SorCS1 isoforms. Traffic *9*, 980–994.

O'Sullivan, M.L., de Wit, J., Savas, J.N., Comoletti, D., Otto-Hitt, S., Yates, J.R., 3rd, and Ghosh, A. (2012). FLRT proteins are endogenous latrophilin ligands and regulate excitatory synapse development. Neuron *73*, 903–910.

Oetjen, S., Mahlke, C., Hermans-Borgmeyer, I., and Hermey, G. (2014). Spatiotemporal expression analysis of the growth factor receptor SorCS3. J. Comp. Neurol. *522*, 3386–3402.

Ollila, H.M., Soronen, P., Silander, K., Palo, O.M., Kieseppä, T., Kaunisto, M.A., Lönnqvist, J., Peltonen, L., Partonen, T., and Paunio, T. (2009). Findings from bipolar disorder genome-wide association studies replicate in a Finnish bipolar family-cohort. Mol. Psychiatry *14*, 351–353.

Poulopoulos, A., Aramuni, G., Meyer, G., Soykan, T., Hoon, M., Papadopoulos, T., Zhang, M., Paarmann, I., Fuchs, C., Harvey, K., et al. (2009). Neuroligin 2 drives postsynaptic assembly at perisomatic inhibitory synapses through gephyrin and collybistin. Neuron *63*, 628–642.

Reitz, C., Tokuhiro, S., Clark, L.N., Conrad, C., Vonsattel, J.P., Hazrati, L.N., Palotás, A., Lantigua, R., Medrano, M., Z Jiménez-Velázquez, I., et al. (2011). SORCS1 alters amyloid precursor protein processing and variants may increase Alzheimer's disease risk. Ann. Neurol. *69*, 47–64.

Sanders, S.J., Murtha, M.T., Gupta, A.R., Murdoch, J.D., Raubeson, M.J., Willsey, A.J., Ercan-Sencicek, A.G., DiLullo, N.M., Parikshak, N.N., Stein, J.L., et al. (2012). De novo mutations revealed by whole-exome sequencing are strongly associated with autism. Nature *485*, 237–241.

Savas, J.N., De Wit, J., Comoletti, D., Zemla, R., Ghosh, A., and Yates, J.R., 3rd. (2014). Ecto-Fc MS identifies ligand-receptor interactions through extracellular domain Fc fusion protein baits and shotgun proteomic analysis. Nat. Protoc. *9*, 2061–2074.

Scheiffele, P., Fan, J., Choih, J., Fetter, R., and Serafini, T. (2000). Neuroligin expressed in nonneuronal cells triggers presynaptic development in contacting axons. Cell *101*, 657–669.

Schwenk, J., Harmel, N., Brechet, A., Zolles, G., Berkefeld, H., Müller, C.S., Bildl, W., Baehrens, D., Hüber, B., Kulik, A., et al. (2012). High-resolution proteomics unravel architecture and molecular diversity of native AMPA receptor complexes. Neuron *74*, 621–633.

Shepherd, J.D., and Huganir, R.L. (2007). The cell biology of synaptic plasticity: AMPA receptor trafficking. Annu. Rev. Cell Dev. Biol. *23*, 613–643.

Siddiqui, T.J., Pancaroglu, R., Kang, Y., Rooyakkers, A., and Craig, A.M. (2010). LRRTMs and neuroligins bind neurexins with a differential code to cooperate in glutamate synapse development. J. Neurosci. *30*, 7495–7506.

Small, S.A., and Petsko, G.A. (2015). Retromer in Alzheimer disease, Parkinson disease and other neurological disorders. Nat. Rev. Neurosci. *16*, 126–132.

Steinberg, F., Gallon, M., Winfield, M., Thomas, E.C., Bell, A.J., Heesom, K.J., Tavaré, J.M., and Cullen, P.J. (2013). A global analysis of SNX27-retromer assembly and cargo specificity reveals a function in glucose and metal ion transport. Nat. Cell Biol. *15*, 461–471.

Südhof, T.C. (2008). Neuroligins and neurexins link synaptic function to cognitive disease. Nature *455*, 903–911.

Taniguchi, H., Gollan, L., Scholl, F.G., Mahadomrongkul, V., Dobler, E., Limthong, N., Peck, M., Aoki, C., and Scheiffele, P. (2007). Silencing of neuroligin function by postsynaptic neurexins. J. Neurosci. *27*, 2815–2824.

Traub, L.M. (2009). Tickets to ride: selecting cargo for clathrin-regulated internalization. Nat. Rev. Mol. Cell Biol. *10*, 583–596.

Wang, X., Zhao, Y., Zhang, X., Badie, H., Zhou, Y., Mu, Y., Loo, L.S., Cai, L., Thompson, R.C., Yang, B., et al. (2013). Loss of sorting nexin 27 contributes to excitatory synaptic dysfunction by modulating glutamate receptor recycling in Down's syndrome. Nat. Med. *19*, 473–480.

Willnow, T.E., Petersen, C.M., and Nykjaer, A. (2008). VPS10P-domain receptors - regulators of neuronal viability and function. Nat. Rev. Neurosci. *9*, 899–909.

Yap, C.C., and Winckler, B. (2012). Harnessing the power of the endosome to regulate neural development. Neuron *74*, 440–451.

Yap, C.C., Wisco, D., Kujala, P., Lasiecka, Z.M., Cannon, J.T., Chang, M.C., Hirling, H., Klumperman, J., and Winckler, B. (2008). The somatodendritic endosomal regulator NEEP21 facilitates axonal targeting of L1/NgCAM. J. Cell Biol. *180*, 827–842.

Zhang, C., Atasoy, D., Araç, D., Yang, X., Fucillo, M.V., Robison, A.J., Ko, J., Brunger, A.T., and Südhof, T.C. (2010). Neurexins physically and functionally interact with GABA(A) receptors. Neuron *66*, 403–416.